Distinct roles for Dectin-1 and Dectin-2 in skin wound healing and neutrophilic inflammatory responses

Kenji Yamaguchi[1] (ORCID: 0000-0003-3313-3048), Emi Kanno[2*] (ORCID: 0000-0003-2339-122X), Hiromasa Tanno[2] (ORCID: 0000-0002-6031-6432), Ayako Sasaki[1] (ORCID: 0000-0002-9261-2359), Yuki Kitai[3] (ORCID: 0000-0003-3271-6807), Takayuki Miura[1] (ORCID: 0000-0002-0437-0880), Naoyuki Takagi[1] (ORCID: 0000-0001-6415-0233), Miki Shoji[1] (ORCID: 0000-0002-2061-5024), Jun Kasamatsu[4] (ORCID: 0000-0001-9718-8377), Ko Sato[4] (ORCID: 0000-0002-5548-6285), Yuka Sato[2] (ORCID: 0000-0003-4234-9617), Momoko Niiyama[2] (ORCID: 0000-0003-0788-2838), Yuka Goto[2] (ORCID: 0000-0002-0874-4819), Keiko Ishii[3] (ORCID: 0000-0003-0794-746X), Yoshimichi Imai[1] (ORCID: 0000-0001-5360-958X), Shinobu Saijo[5] (ORCID: 0000-0002-3802-8821), Yoichiro Iwakura[6] (ORCID: 0000-0002-9934-5775), Masahiro Tachi[1] (ORCID: 0000-0003-2993-3202), Kazuyoshi Kawakami[3, 4] (ORCID: 0000-0001-6599-1915)

[1]Department of Plastic and Reconstructive Surgery, Tohoku University Graduate School of Medicine, 2-1 Seiryo-cho, Aoba-ku, Sendai, Japan

[2]Department of Science of Nursing Practice, Tohoku University Graduate School of Medicine, 2-1 Seiryo-cho, Aoba-ku, Sendai, Japan

[3]Department of Medical Microbiology, Mycology and Immunology, Tohoku University Graduate School of Medicine, 2-1 Seiryo-cho, Aoba-ku, Sendai, Japan

[4]Department of Intelligent Network for Infection Control, Tohoku University Graduate School of Medicine, 2-1 Seiryo-cho, Aoba-ku, Sendai, Japan

[5]Department of Molecular Immunology, Medical Mycology Research Center, Chiba University, 1-8-1 Inohana, Chuo-ku, Chiba, Japan

[6]Division of Laboratory Animals, Research Institute for Biomedical Sciences, Tokyo University of Science, 2669 Yamazaki, Noda, Chiba, Japan

Number of figures: *6*

Number of supplemental figures: *8*

Corresponding author: Emi Kanno, RN, PhD

Department of Science of Nursing Practice, Tohoku University Graduate School of Medicine

2-1 Seiryo-cho, Aoba-ku, Sendai, Miyagi 980-8575, Japan

Phone: +81-22-717-8675; Fax: +81-22-717-7910

Email: ekanno@med.tohoku.ac.jp

***Short Title*: Dectin-1 and Dectin-2 in wound healing**

***Abbreviations used*:** *WT, wild type; PCNA, proliferating cell nuclear antigen; α-SMA, α-smooth muscle actin; CLR, C-type lectin receptor; DAMPs, damage-associated molecular patterns; PAMPs, pathogen-associated molecular patterns; PBS, phosphate buffered saline; TGF, transforming growth factor; VEGF, vascular endothelial growth factor; EGF, epidermal growth factor; Dectin, dendritic-cell-associated C-type lectin; NETs, neutrophil extracellular traps; TNF, tumor necrosis factor; TLR, toll-like receptor; MIP, macrophage inflammatory protein; KC, keratinocyte-derived chemokine; MMP, matrix metalloproteinase*

***Key words*:** Dectin-1, Dectin-2, wound healing, neutrophils, NETosis

Abstract

C-type lectin receptors (CLRs) recognize microbial polysaccharides. The CLRs Dectin-1 and Dectin-2, which are triggered by β-glucan and α-mannan, respectively, contribute to up-regulation of the inflammatory response. Recently, we demonstrated that activation of the Dectin-2 signal delayed wound healing; in previous studies, triggering the Dectin-1 signal promoted this response. However, the precise roles of these CLRs in skin wound healing remain unclear. This study was conducted to determine the roles of Dectin-1 and Dectin-2 in skin wound healing, with a particular focus on the kinetics of neutrophilic inflammatory response. Full-thickness wounds were created on the backs of C57BL/6 mice, and the effects of Dectin-1 or Dectin-2 deficiency and those of β-glucan or α-mannan administration were examined. We also analyzed wound closure, histological findings, and neutrophilic inflammatory response including neutrophil extracellular trap (NET) formation at the wound sites. We found that Dectin-1 contributed to the acceleration of wound healing by inducing early-phase neutrophil accumulation, whereas Dectin-2 was involved in prolonged neutrophilic responses and NET formation, leading to delayed wound healing. Dectin-2 deficiency also improved collagen deposition and TGF-β1 expression. These results suggest that Dectin-1 and Dectin-2 have different roles in wound healing through their different effects on the neutrophilic response.

(*Word count*: 199)

INTRODUCTION

Skin wounds normally heal through an efficient process that is characterized by inflammation, proliferation, and remodeling. Many cell types, including neutrophils, macrophages, and fibroblasts, are involved in orchestrating the healing process. The inflammatory response causes these cells to secrete several cytokines and growth factors that work together to induce cell migration and remodeling (Pasparakis et al., 2014). Pathogen-associated molecular patterns (PAMPs) and damage-associated molecular patterns (DAMPs) trigger these responses upon being recognized by pattern recognition receptors (PRRs) such as C-type lectin receptors (CLRs) (Girardin et al., 2002, Yan et al., 2017).

CLRs are well known for playing key roles in the host defense against fungal pathogens, mostly by recognizing pathogens' cell wall polysaccharides such as β-glucan and α-mannan (Saijo and Iwakura, 2011). Dectin-1 and Dectin-2 contribute to inflammatory responses via activation of NF-kappa B and are triggered by β-glucan and α-mannan, respectively. Additionally, Dectin-1 binds to the endogenous intermediate filament protein vimentin (Thiagarajan et al., 2013), while Dectin-2 interacts with the endogenous protein β-glucuronidase (Mori et al., 2017). Although it is not well understood how CLRs contribute to wound healing, we recently demonstrated that CARD9, an essential signaling adaptor molecule that is triggered by CLRs, was involved in these responses (Kanno et al., 2017). We also found that Dectin-2-mediated signaling led to delayed wound healing through prolonged neutrophilic inflammatory response and accompanying NET formation (Miura et al., 2019). Additionally, administration of β-glucan was reported to improve wound healing (Palma et

al., 2006), although it remains unclear how Dectin-1 deficiency affects the neutrophilic responses at wound sites.

Neutrophils, the first responder cells in skin injury, are recruited through the influence of chemokines and cytokines such as keratinocyte-derived chemokine (KC) and tumor necrosis factor (TNF)-α. However, only limited information is available about the role of neutrophils in wound healing (Pasparakis et al., 2014). Infiltrating neutrophils play central roles in debridement and anti-microbial defense through phagocytosis and NET formation, a process called NETosis (Kolaczkowska and Kubes, 2013). However, prolonged neutrophil activation is known to cause intractable wounds (Kolaczkowska and Kubes, 2013, de Oliveira et al., 2016). Previously, Wong and co-workers revealed that neutrophils isolated from diabetic humans and mice were susceptible to NETosis when stimulated with the $Ca2^{+}$ ionophore ionomycin, and that the NETs resulted in impaired wound healing (Wong et al., 2015). Additionally, it was reported that bacterial endotoxin lipopolysaccharide (LPS) and α-mannan promoted NETs (Brinkmann et al., 2004; Miura et al., 2019) and that TNF-α primed neutrophils, making them more susceptible to NETosis (Thomas et al., 2012). These earlier observations suggested that NETosis may play an unknown physiological role in the process. It consistent with this possibility that TNF-α is quickly produced in the early phase of wound healing even under uninfected conditions (Kanno et al., 2011).

Based on this background, in the present study, we conducted comparative analyses to define the roles of Dectin-1 and Dectin-2 in wound healing, with particular emphasis on the kinetics of neutrophilic inflammatory responses and NET formation, using mice that were deficient in these CLRs. Here, we found that Dectin-1 contributed to the acceleration of

wound healing through inducing early phase neutrophil accumulation, whereas Dectin-2 was involved in the prolonged neutrophilic inflammatory response and NETs, which may play a particular role in the regulation of excessive healing response.

RESULTS

Different kinetics for Dectin-1 and Dectin-2 expression in skin after wounding

To identify the contributions of Dectin-1 and Dectin-2, the expression of these molecules' mRNA was examined. Dectin-1 was rapidly expressed, appearing at 3 hours, peaking at 6 hours, and quickly declining thereafter to the baseline level. Dectin-2, however, appeared at 6 hours, peaked at 12 or 24 hours, and remained somewhat elevated for up to 7 days (Figure 1a). In immunohistochemical analysis, both Dectin-1 and Dectin-2 were detected in infiltrating leukocytes and fibroblasts in the early phase after wounding, but they were not detected in unwounded skin; additionally, the reported endogenous ligands for Dectin-1 (vimentin) (Thiagarajan et al., 2013) and Dectin-2 (β-glucuronidase) (Mori et al., 2017) were also detected around the cells expressing these receptors (Figure 1b). As shown in Figure 1c, both Dectin-1 and Dectin-2 were apparently expressed in neutrophils, macrophages, and fibroblasts at 24 hours and also on day 5, although the expression was lower in these cells (Supplementary Figure S1). We also confirmed that the supernatants, which were collected from wounds that contained molecules that activated signaling that was mediated via Dectin-1 or Dectin-2 using NFAT-GFP reporter assays (Supplementary Figure S2), and we confirmed that GFP is expressed in Dectin-2-expressing reporter cells but not in Dectin-1-expressing reporter cells.

Distinct effects of Dectin-1 and Dectin-2 deficiency on wound healing

To elucidate the distinct roles of Dectin-1 and Dectin-2, we examined the effects of Dectin-1 and Dectin-2 deficiency using Dectin-1 knockout (KO) and Dectin-2KO mice. As shown in

Figure 2a and b, wound closure was significantly impaired in Dectin-1KO mice but it was enhanced in Dectin-2KO mice compared with WT mice. In Dectin-1KO mice, the re-epithelialization rate was significantly decreased compared with WT and Dectin-2KO mice; in Dectin-2KO mice, however, the re-epithelialization rate was significantly increased (Figure 2c). As alternate indicators of wound healing, we evaluated proliferating cell nuclear antigen (PCNA), CD31, and α-smooth muscle actin (α-SMA), which indicate epithelial cell differentiation, vascularization, and myofibroblast differentiation, respectively. As shown in Figure 2d, the counts of PCNA-positive epidermal cells were significantly decreased in Dectin-1KO mice compared with WT and Dectin-2KO mice. CD31-positive vessel counts were markedly decreased in Dectin-1KO mice and enhanced in Dectin-2KO mice compared with WT mice (Figure 2e). Dectin-2 deficiency led to an increase in α-SMA-positive cell numbers (Figure 2f).

Because neutrophils play a critical role in inflammatory responses (Wilgus et al., 2013), we examined the effects of Dectin-1 and Dectin-2 deficiency on neutrophil accumulation. As shown in Figure 2g, the neutrophil counts were significantly lower in Dectin-1KO mice compared with WT mice at 6 hours, whereas the opposite results were obtained in Dectin-2KO mice. On day 5, the neutrophil counts remained markedly decreased in Dectin-2KO mice.

Distinct effects of Dectin-1- and Dectin-2-mediated activation on wound healing

We next evaluated how Dectin-1- and Dectin-2-activation affected wound healing. We examined the effects of administration of either dZymosan (containing β-glucans, a known

Dectin-1 ligand) or α-mannan (a known Dectin-2 ligand). As shown in Figure 3a and b, WT mice treated with dZymosan showed significant acceleration of wound closure, whereas treatment with α-mannan led to a significant delay in wound closure compared with mice treated with vehicle control. These responses were canceled in CARD9KO mice (Supplementary Figure S3). Similar results were obtained using Furfurman (another Dectin-2 ligand) instead of α-mannan (Supplementary Figure S4). In dZymosan-treated mice, the re-epithelialization rate was significantly increased compared with vehicle-treated mice, whereas treatment with α-mannan led to delayed re-epithelialization (Figure 3c). Additionally, the hydroxyproline content was significantly decreased in α-mannan-treated mice compared with vehicle- or dZymosan-treated mice (Figure 3d). As shown in Figure 3e–g, the PCNA, CD31, and α-SMA-positive cell counts were significantly increased in dZymosan-treated mice, whereas the opposite results were obtained in α-mannan-treated mice.

Effect of topical dZymosan or α-mannan administration on neutrophilic inflammatory responses and NETosis

To elucidate the effects of dZymosan and α-mannan on neutrophilic responses, we examined the kinetics of neutrophil accumulation. The proportions of neutrophils, defined as $CD45^+CD11b^+Ly6G^+$ cells, were evaluated by flow cytometry. In mice treated with dZymosan, neutrophil counts were increased in the early phases compared with other groups, but the counts had returned to baseline levels on day 3. In mice treated with α-mannan, however, neutrophil counts were equivalent to those in the other groups for the first 24 hours, then markedly increased starting on day 3 and peaking on day 5. In vehicle-treated mice,

neutrophil counts returned to baseline levels by day 3 (Figure 4a). We confirmed these findings through immunohistochemical analysis (Supplementary Figure S5). The increase in neutrophil counts caused by dZymosan at 6 hours and by α-mannan on day 5 were inhibited in Dectin-1KO mice and Dectin-2KO mice, respectively (Supplementary Figure S6). Additionally, KC and MIP-2 synthesis rates were significantly higher at 6 hours in the dZymosan-treated group compared with the other groups, but were higher on day 3 in the α-mannan-treated group compared with the other groups. TNF-α and interleukin (IL)-17A levels were not different among these groups at 6 hours, but were significantly higher in the α-mannan-treated group on day 3 (Figure 4b). Similar results were obtained regarding leukocyte and macrophage accumulation (Supplementary Figure S7). To clarify the effect of Dectin-1 activation, NETs were evaluated in mice treated with dZymosan. As shown in Figure 4c, in contrast to α-mannan treatment, dZymosan treatment did not increase co-localized Cit H3 and Ly6G expression compared with vehicle. Western blotting analysis similarly revealed that dZymosan treatment did not increase Cit H3 expression, whereas α-mannan treatment led to a striking increase on day 5 (Figure 4d and e), but not at 6 hours (Figure 4f).

Effects of Dectin-1 and Dectin-2 deficiency, DNase, and neutrophil depletion on NETosis

To address this possibility, we examined NETs under natural conditions without any treatments. As shown in Figure 5a, Cit H3 expression began to increase at 6 hours, reached its peak on day 3, and then began to decrease, although its levels remained higher compared with those in unwounded skin tissues through day 10. Thus, we examined the effects of Dectin-1 and Dectin-2 deficiency on NETs. In Dectin-2KO mice, Cit H3 expression was significantly

lower compared with WT mice (Figure 5b), whereas there was no significant difference between Dectin-1KO and WT mice (Figure 5c). A previous study reported that DNase 1 administration promoted wound healing (Wong et al., 2015), although its effect on NETosis remains to be clarified. As shown in Figure 5d, DNase 1 administration significantly reduced the delay in wound closure in WT mice that were treated with α-mannan, while no such effect was seen in wounds that were not treated with either ligand. On day 3, however, untreated wound closure was significantly accelerated by DNase 1 administration (Figure 5e).

We then examined the effect of DNase 1 treatment on NETosis in wound tissues that were treated or not treated with α-mannan. As shown in Figure 5f, this treatment had no significant effect on Cit H3 expression, although Cit H3 expression tended to be higher in untreated wounds. Next, we used anti-Gr-1 mAb to examine the effect of neutrophil depletion on wound closure and NETs in WT mice. As shown in our recent study (Miura et al., 2019), neutrophils were completely depleted by this treatment. Thus, wound closure was significantly accelerated in mice treated with anti-Gr-1 mAb compared with control IgG-treatment (Figure 5g), which supports our hypothesis. Additionally, anti-Gr-1 mAb administration resulted in a significant reduction in Cit H3 expression compared with control (Figure 5h).

Effect of Dectin-2 deficiency on wound maturation

To further clarify the effect of Dectin-2 on late-phase events in wound healing, we examined the effect of Dectin-2 deficiency on collagen deposition and matrix metalloproteinase (MMP) expression. As shown in Figure 6a, the content of hydroxyproline, a collagen-specific amino

acid, was significantly increased in Dectin-2-deficient mice compared with WT mice. Additionally, the COL3A1-to-COL1A1 ratio tended to be lower in Dectin-2KO mice compared with WT mice (Figure 6b). Transforming growth factor (TGF)-β1 expression was also increased in Dectin-2KO compared with WT mice (Figure 6c). MMP-2 and MMP-8 expression levels and the neutrophil elastase activity level were markedly decreased in Dectin-2-KO compared with WT mice (Figure 6d and e).

DISCUSSION

In the current study, we demonstrated that Dectin-1 deficiency impaired wound healing while Dectin-1 activation accelerated wound healing through promoting early-phase neutrophil accumulation. However, Dectin-2 was involved in the prolonged neutrophilic inflammatory response that is associated with NET accumulation. Additionally, Dectin-2 activation delayed wound healing and attenuated both collagen synthesis and TGF-β expression. Recently, we demonstrated that Dectin-2-mediated signaling delayed wound healing by prolonging neutrophilic responses with NETosis (Miura et al., 2019). However, the effect of Dectin-1-mediated signaling on wound healing was unknown. Thus, to our best knowledge, no studies have previously reported the involvement of Dectin-1 and Dectin-2 in the regulation of skin wound healing in distinct ways, especially in the neutrophil response.

Both Dectin-1 and Dectin-2 are known to be expressed on keratinocytes, dendritic cells, Langerhans cells, macrophages, and neutrophils (van den Berg et al., 2014, Brasch et al., 2014, Taylor et al., 2007, Taylor et al., 2005). To our knowledge previously unreported that these CLRs are also expressed on fibroblasts. Thus, both Dectin-1 and Dectin-2 are likely to be similarly expressed on recruited leukocytes and fibroblasts. However, Taylor and co-workers (Taylor et al., 2005) have previously revealed that Dectin-1 is expressed at high levels on early inflammatory monocytes, whereas Dectin-2 is expressed on migrated inflammatory monocytes in the late phases of wound healing. Taylor et al. (2005) also detected high levels of Dectin-1 expression on the surfaces of tissue-resident macrophages and resident peritoneal macrophages, whereas Dectin-2 expression was very low in these resident cells. In the present study, in the early inflammatory phase, we found that the

proportions of Dectin-1- and Dectin-2-expressing macrophages were 30.2%±0.8% and 19.3±1.6%, respectively. Thus, these data suggest that Dectin-1 may be highly expressed on early inflammatory macrophages and skin tissue-resident macrophages.

Both Dectin-1 and Dectin-2 play central roles in host defense against a fungal infection through recognition of β-1,3-glucan and high-mannose structures, respectively (Gantner et al., 2003, McGreal et al., 2006). However, it remains unclear whether vimentin, an endogenous binding protein for Dectin-1 (Thiagarajan et al., 2013), and β-glucuronidase, an endogenous binding protein for Dectin-2 (Mori et al., 2017), are involved in the induction of inflammatory responses after interacting with their receptors. In this study, vimentin and β-glucuronidase were detected near Dectin-1- and Dectin-2-expressing cells. Consistent with this possibility, experiments with reporter cells revealed that the supernatants of wounded tissues activate Dectin-2-mediated but not Dectin-1-mediated signaling. Thus, our findings suggest that some endogenous ligands such as β-glucuronidase may be involved in Dectin-2-mediated responses. The supernatants from wounds did not activate Dectin-1 reporter cells in this study. Previously, Xu and co-workers demonstrated that secreted forms of vimentin are structurally different from non-secreted forms (Xu et al., 2004), which suggests that secreted vimentin, despite being a putative Dectin-1 ligand, may interact less readily with Dectin-1 in wounded tissue. However, it cannot be ruled out that this putative Dectin-1 ligand may simply be secreted for a very short time after wounding.

We present evidence indicating that Dectin-1 regulates early-phase neutrophilic responses, which are dependent on KC and MIP-2 production, whereas Dectin-2 is involved in regulating late-phase neutrophilic responses, which are associated with these chemokines

and TNF-α and IL-17A. In a previous study using a keratitis mouse model, β-glucan from *Aspergillus fumigatus* was shown to stimulate Dectin-1 signaling in resident corneal macrophages, thereby accelerating neutrophil recruitment by inducing KC production (Leal et al., 2010). Additionally, Fan et al. (2019) recently demonstrated that Dectin-1 on macrophages contributes to early phase neutrophil recruitment, which is associated with increased KC production, and that Dectin-1 expression levels subsequently decline to baseline levels within 72 h after myocardial ischemia–reperfusion injury. Considered collectively, the available findings suggest that Dectin-1 expressed on resident cells such as macrophages may largely contribute to early phase neutrophil accumulation by sensing early damage signals and inducing chemokine production.

The current study indicated that late-phase neutrophilic responses and NET formation are attenuated under Dectin-2-deficiency. Dectin-2 is strongly expressed on migrated inflammatory monocytes (Taylor et al., 2005), and macrophages are maintained at infarcted sites for 7 days after myocardial infarction (Yan et al., 2017). Consistent with these observations, we also observed that low but significant levels of Dectin-2 were detected until day 7 after wounding. Because α-mannan induced late-phase neutrophilic responses, it is likely that β-glucuronidase from damaged tissues is involved in similar responses. Additionally, TNF-α and IL-17A synthesis were significantly higher in the late phase after α-mannan treatment. Both TNF-α and IL-17A are well-known inducers of neutrophil recruitment (Maher et al., 2013) and triggers of excessive NETosis (Khandpur et al., 2013), although TNF-α is also involved in the disappearance of neutrophils through apoptosis (Degterev and Yuan, 2008). The decrease in early neutrophil apoptosis that is associated with

reduced TNF-α production is involved in prolonging neutrophil infiltration and enhancing NETs (Gray et al., 2018). Thus, in the present study, the failure of neutrophils to disappear might be caused by their attenuated apoptosis in the early phase and might also be involved in the NETs through TNF-α and IL-17A. Consistent with this possibility, our previous study reported prolonged neutrophil accumulation and a corresponding reduction in neutrophil apoptosis in wound tissues in mice that were deficient in NKT cells (Tanno et al., 2017).

Taylor and coworkers showed that both complement and Dectin-1 are considered to be "*primary pathogen recognition systems*" because both are characterized by links between pathogens and leukocytes in the immune responses to fungal infection (McDonald et al., 2012, Taylor et al., 2007). In most fungal pathogens, the inner cell wall polysaccharides, including β-glucan and chitin, are covered by outer cell wall polysaccharides such as mannans, which are accordingly recognized by CLRs, leading to the development of immune responses (Erwig and Gow, 2016). The exposure condition for β-glucans on the surface is different between yeasts and hyphae of *Candida albicans*. When surface polysaccharide structures change from those of mildly virulent yeasts to those of highly virulent hyphae depending on the invasion status in the host, the resulting change in the access of Dectin-1 to the inner β-glucan structures may affect the neutrophilic responses (Gow et al., 2011). Additionally, immune responses became more pronounced upon exposure of the host PRRs to β-glucan as opposed to α-mannan (Erwig and Gow, 2016, Netea et al., 2006). In the present study, we demonstrated that Dectin-1 expression increases quite rapidly, enabling it to play major roles in the regulation of early phase neutrophil accumulation. Thus, Dectin-1 could be considered to be a central player in the early phase of wound healing through its direct

interaction with an unknown putative endogenous ligand such as vimentin (Thiagarajan et al., 2013) as well as with exogenous ligands that are derived from resident fungi such as β-glucan (Gao et al. 2010). Previously, Mor-Vaknin et al. (Mor-Vaknin et al., 2003) revealed that vimentin is secreted from activated macrophages upon stimulation with TNF-α. Our previous study indicated that TNF-α is released shortly after wounding and that it promotes inflammatory leukocyte recruitment (Kanno et al., 2011). Considered collectively, these findings suggest that a regulatory mechanism that is promoted by TNF-α may be involved in the early events of wound healing after being triggered by a Dectin-1-dependent signaling pathway.

In the current study, Dectin-1 expression quickly decreased to baseline levels beginning 12 h after wounding, whereas Dectin-2 expression continued to gradually increase during this period. It has been reported that Dectin-1 and Dectin-2 are not detected at the same time points, and that Dectin-2 expression is up-regulated in monocytes/macrophages under Dectin-1-deficient conditions (Taylor et al., 2005). Additionally, Dectin-2 usually forms heterodimers with MCL to enable more effective recognition of their ligands (Zhu et al., 2013), and these heterodimers act to inhibit Dectin-1 signaling via Mincle, another member of the CLRs (Wevers et al., 2014). Thus, in the current model, cross-regulation between Dectin-1 and Dectin-2 may affect each of their expressions, and the presence of the Dectin-2-MCL complex may contribute to the quick decrease in Dectin-1 expression through a direct or indirect mechanism.

In this study, we found that NETs reached their peak level on day 3 in a Dectin-2-dependent, but not Dectin-1-dependent, manner during natural wound healing in absence of

exogenous ligands. Previously, Wong et al. (Wong et al., 2015) revealed that NETs are mediated by peptidylarginine deiminase 4 (PAD4), a calcium-dependent enzyme, during natural wound healing (Luo et al., 2006). Calcium dependence was also reported in Dectin-2 binding to its ligand (Sato et al., 2006). In agreement with these observations, calcium flux was reported to be necessary for efficient NETs (Gupta et al., 2014), and NETosis was reported to be induced by incubation with ionomycin, a calcium ionophore (Wong et al., 2015). In previous studies, wound closure was accelerated, but dermal healing was not affected by partial depletion of neutrophils by approximately 80% for 2 days (Dovi et al., 2003). However, in the present study, complete neutrophil depletion resulted in a significant reduction of NETs formation and an acceleration of wound closure, which suggests that NETs-forming neutrophils may be involved in interference with the wound healing process, including that in dermis.

We also observed that DNA in the NETs plays a suppressive role as evidenced by the finding that DNase I treatment promotes wound closure under both natural and α-mannan-treated conditions. Similar findings have been reported previously (Wong et al., 2015). These results suggest that DNA or its associated enzymes including elastase (Urban et al., 2009) may be involved in the suppressive effect of NETs against wound healing. Neutrophil elastase, which has been reported to bind to DNA in NETs (Papayannopoulos et al., 2010), may play a role in this suppressive effect because, in our recent study, treatment with neutrophil elastase improved the delayed wound healing caused by activation of Dectin-2 signals (Miura et al., 2019). Consistent with this possibility, in the present study, lower levels of neutrophil elastase were detected in Dectin-2KO mice compared with WT mice.

Additionally, MMP-8 expression in wound tissues was also lower in Dectin-2KO mice. Considered collectively, our current results suggest that some MMPs may be involved in late-phase regulation of wound healing via a Dectin-2-dependent mechanism.

Scarring in the skin after trauma or surgery has been a major medical problem, and the mechanisms of scarring have received much attention. Novel approaches for keloids and hypertrophic scars seek to treat these scar tissues as chronic inflammatory disorders of the skin (Gauglitz et al., 2011, Ogawa, 2017). High levels of TGF-β1, which is a downstream factor in inflammation, are detected at scar tissues, and markedly improved scarring is reported under TGF-β1-deficient conditions (Ferguson and O'Kane, 2004). TGF-β1 is well known as a promoting factor for collagen synthesis from fibroblasts and also contributes to collagen-type transition from immature type III collagen (encoded by *COL3A1*) to mature type I collagen (encoded by *COL1A1*) (Kim et al., 2018). For a long time, the detailed mechanisms of scarring have remained unclear because the mechanisms inhibiting the healing process have not been elucidated. In this study, TGF-β synthesis and collagen-type transition from COL1A3 to COL1A1 were promoted under Dectin-2-deficient conditions. These results suggest that Dectin-2-dependent signaling may prevent excessive collagen deposition, which leads to scar formation, through regulating TGF-β and collagen-type transition.

We also observed delayed wound closure in WT mice treated with α-mannan, which was accompanied by prolonged neutrophilic inflammation and TNF-α production, compared with those treated with dZymosan or vehicle control. Previously, we demonstrated that inoculation of *Pseudomonas aeruginosa* at wounded skin accelerated re-epithelialization and neovascularization on day 3 as well as local infiltration of neutrophils, though no significant

acceleration of wound healing was detected on days 7 and 10 (Kanno et al., 2011). In addition, high concentration of TNF-α, mainly derived from neutrophils, were detected from 6 hours to day 7 after this bacterial inoculation. Thus, considering our current and previous findings collectively, TNF-α might play a promoting role in the early phase and inhibitory role in the late phase of wound healing. Further investigations are necessary to address this unsolved issue.

In conclusion, the current study may provide a new insight into how Dectin-2 helps to prevent an excessive wound healing response, followed by scar formation, by playing a key role in negative regulation of the wound healing response. This suggests a possible target for developing novel therapies to treat chronic wounds, such as diabetic leg ulcers, and to prevent keloids. These points are summarized in Supplementary Figure S8. Additionally, Dectin-1 could be another target molecule for developing novel therapies to accelerate wound healing by promoting the inflammatory response.

MATERIALS AND METHODS

An extended description of our materials and methods can be found in the Supplementary Materials and Methods online.

Mice

Dectin-1 KO mice were generated by homologous recombination of the Clec7a gene as described previously (Saijo and Iwakura, 2011) and backcrossed to C57BL/6 mice for eight generations. Dectin-2 gene-disrupted (knockout [KO]) mice were generated by homologous recombination of the Clec4n gene as described previously (Saijo et al., 2010) and backcrossed to C57BL/6 mice for seven generations or for more than eight generations. CARD9 KO mice were generated and established as described previously (Hara et al., 2007) and backcrossed to C57BL/6 mice for more than eight generations. Wild-type (WT) littermate mice of Dectin-2KO mice were used as controls for seven generations. Except for experiments with Dectin-2KO mice that were established over seven generations, C57BL/6 mice purchased from CLEA Japan (Tokyo, Japan) were used as WT control. All mice were kept under specific pathogen-free conditions in the Institute for Animal Experimentation, Tohoku University Graduate School of Medicine (Sendai, Japan).

Wound creation and tissue collection

Wound creation and tissue collection were performed as described in the Supplementary Materials and Methods.

Treatment with dZymosan (zymosan depleted) or α-mannan

Treatment with dZymosan (zymosan depleted) or α-mannan were performed as described in the Supplementary Materials and Methods.

Data availability statement

No data sets were generated or analyzed during this study.

CONFLICT OF INTEREST

The authors state that there are no conflicts of interest.

ACKNOWLEDGMENTS

We thank Dr. Sho Yamasaki (Department of Molecular Immunology, Research Institute for Microbial Diseases, Osaka University) for providing us with Dectin-1 and Dectin-2 reporter cells and Dr. Hiromitsu Hara (Department of Immunology, Graduate School of Medical and Dental Sciences, Kagoshima University) for providing us with the CARD9KO mice.

This work was supported in part by a Grant-in-Aid for Scientific Research (C) (18K09473), Grant-in-Aid for Scientific Research (B) (19H03812), a Grant-in-Aid for Challenging Exploratory Research (19K22649), and a Grant-in-Aid for Young Scientists (19K19494) from the Ministry of Education, Culture, Sports, Science and Technology of Japan.

AUTHOR CONTRIBUTIONS

Conceptualization: KY, EK, MT, KK; Data curation: KY, EK, HT, KK; Formal Analysis: KY, EK, HT, AY, YK; Funding Acquisition: EK, MT, MT, KK; Investigation: KY, HT, TM, NT, MS, JK, KS, YS, MN, YG, KI; Methodology: KY, HT, JK, KS, YI; Project Administration: KY, EK, KK; Resources: KY, EK, HT, SS, YI, KK; Supervision: EK, MT, KK; Validation: KY, EK, HT, KK; Visualization: TK, EK, MT, KK; Writing-Original Draft Preparation: KY, EK, KK; Writing-Review and Editing: KY, EK, and KK.

REFERENCES

van den Berg, L.M., Zijlstra-Willems, E.M., Richters, C.D., Ulrich, M.M.W., Geijtenbeek, T.B.H. **Dectin-1 activation induces proliferation and migration of human keratinocytes enhancing wound re-epithelialization.** Cell. Immunol. 2014;289(1–2):49–54

Brasch, J., Mörig, A., Neumann, B., Proksch, E. **Expression of antimicrobial peptides and toll-like receptors is increased in tinea and pityriasis versicolor.** Mycoses. 2014;57(3):147–52

Brinkmann, V., Reichard, U., Goosmann, C., Fauler, B., Uhlemann, Y., Weiss, D.S. et al. **Neutrophil extracellular traps kill bacteria.** Science. 2004;303(5663):1532–5

Degterev, A., Yuan, J. **Expansion and evolution of cell death programmes.** Nat. Rev. Mol. Cell Biol. 2008;9(5):378–90

Dovi, J.V., He, L-K., DiPietro, L.A. **Accelerated wound closure in neutrophil-depleted mice.** J. Leukoc. Biol. 2003;73(4):448–55

Erwig, L.P., Gow, N.A.R. **Interactions of fungal pathogens with phagocytes.** Nat. Rev. Microbiol. 2016;14(3):163–76

Fan, Q., Tao, R., Zhang, H., Xie, H., Lu, L., Wang, T. et al. **Dectin-1 contributes to**

myocardial ischemia/reperfusion injury by regulating macrophage polarization and neutrophil infiltration. Circulation. 2019;139(5):663–78

Ferguson, M.W.J., O'Kane, S. **Scar-free healing: from embryonic mechanisms to adult therapeutic intervention.** Philos. Trans. R. Soc. Lond. B. Biol. Sci. 2004;359(1445):839–50

Gantner, B.N., Simmons, R.M., Canavera, S.J., Akira, S., Underhill, D.M. **Collaborative induction of inflammatory responses by dectin-1 and Toll-like receptor 2.** J. Exp. Med. 2003;197(9):1107–17

Gao, Z., Perez-Perez, G.I., Chen, Y., Blaser, M.J. **Quantitation of major human cutaneous bacterial and fungal populations.** J. Clin. Microbiol. 2010;48(10):3575–81

Gauglitz, G.G., Korting, H.C., Pavicic, T., Ruzicka, T., Jeschke, M.G. **Hypertrophic scarring and keloids: pathomechanisms and current and emerging treatment strategies.** Mol. Med. Camb. Mass. 2011;17(1–2):113–25

Girardin, S.E., Sansonetti, P.J., Philpott, D.J. **Intracellular vs extracellular recognition of pathogens--common concepts in mammals and flies.** Trends Microbiol. 2002;10(4):193–9

Gow, N.A.R., van de Veerdonk, F.L., Brown, A.J.P., Netea, M.G. **Candida albicans morphogenesis and host defence: discriminating invasion from colonization.** Nat. Rev. Microbiol. 2011;10(2):112–22

Gray, R.D., Hardisty, G., Regan, K.H., Smith, M., Robb, C.T., Duffin, R. et al. **Delayed neutrophil apoptosis enhances NET formation in cystic fibrosis.** Thorax. 2018;73(2):134–44

Gupta, A.K., Giaglis, S., Hasler, P., Hahn, S. **Efficient neutrophil extracellular trap induction requires mobilization of both intracellular and extracellular calcium pools and is modulated by cyclosporine A.** PloS One. 2014;9(5):e97088

Hara, H., Ishihara, C., Takeuchi, A., Imanishi, T., Xue, L., Morris, S.W. et al. **The adaptor protein CARD9 is essential for the activation of myeloid cells through ITAM-associated and Toll-like receptors.** Nat. Immunol. 2007;8(6):619–29

Kanno, E., Kawakami, K., Ritsu, M., Ishii, K., Tanno, H., Toriyabe, S. et al. **Wound healing in skin promoted by inoculation with Pseudomonas aeruginosa PAO1: The critical role of tumor necrosis factor-α secreted from infiltrating neutrophils.** Wound Repair Regen. 2011;19(5):608–21

Kanno, E., Kawakami, K., Tanno, H., Suzuki, A., Sato, N., Masaki, A. et al. **Contribution of**

CARD9-mediated signalling to wound healing in skin. Exp. Dermatol. 2017;26(11):1097–104

Khandpur, R., Carmona-Rivera, C., Vivekanandan-Giri, A., Gizinski, A., Yalavarthi, S., Knight, J.S. et al. **NETs are a source of citrullinated autoantigens and stimulate inflammatory responses in rheumatoid arthritis.** Sci. Transl. Med. 2013;5(178):178ra40

Kim, K.K., Sheppard, D., Chapman, H.A. **TGF-β1 signaling and tissue fibrosis.** Cold Spring Harb. Perspect. Biol. 2018;10(4)

Kolaczkowska, E., Kubes, P. **Neutrophil recruitment and function in health and inflammation.** Nat. Rev. Immunol. 2013;13(3):159–75

Leal, S.M., Cowden, S., Hsia, Y-C., Ghannoum, M.A., Momany, M., Pearlman, E. **Distinct roles for Dectin-1 and TLR4 in the pathogenesis of Aspergillus fumigatus keratitis.** PLoS Pathog. 2010;6:e1000976

Luo, Y., Arita, K., Bhatia, M., Knuckley, B., Lee, Y-H., Stallcup, M.R. et al. **Inhibitors and inactivators of protein arginine deiminase 4: functional and structural characterization.** Biochemistry. 2006;45(39):11727–36

Maher, B.M., Mulcahy, M.E., Murphy, A.G., Wilk, M., O'Keeffe, K.M., Geoghegan, J.A. et al. **Nlrp-3-driven interleukin 17 production by γδT cells controls infection outcomes during Staphylococcus aureus surgical site infection.** Infect. Immun. 2013;81(12):4478–89

McDonald, J.U., Rosas, M., Brown, G.D., Jones, S.A., Taylor, P.R. **Differential dependencies of monocytes and neutrophils on dectin-1, dectin-2 and complement for the recognition of fungal particles in inflammation.** PloS One. 2012;7(9):e45781

McGreal, E.P., Rosas, M., Brown, G.D., Zamze, S., Wong, S.Y.C., Gordon, S. et al. **The carbohydrate-recognition domain of Dectin-2 is a C-type lectin with specificity for high mannose.** Glycobiology. 2006;16(5):422–30

Miura, T., Kawakami, K., Kanno, E., Tanno, H., Tada, H., Sato, N. et al. **Dectin-2-mediated signaling leads to delayed skin wound healing through enhanced neutrophilic inflammatory response and neutrophil extracellular trap formation.** J. Invest. Dermatol. 2019;139(3):702–11

Mori, D., Shibata, K., Yamasaki, S. **C-type lectin receptor dectin-2 binds to an endogenous protein β-glucuronidase on dendritic cells.** PLOS ONE. 2017;12(1):e0169562

Mor-Vaknin, N., Punturieri, A., Sitwala, K., Markovitz, D.M. **Vimentin is secreted by activated macrophages.** Nat. Cell Biol. 2003;5(1):59–63

Netea, M.G., Gow, N.A.R., Munro, C.A., Bates, S., Collins, C., Ferwerda, G. et al. **Immune sensing of Candida albicans requires cooperative recognition of mannans and glucans by lectin and Toll-like receptors.** J. Clin. Invest. 2006;116(6):1642–50

Ogawa, R. **Keloid and hypertrophic scars are the result of chronic inflammation in the reticular dermis.** Int. J. Mol. Sci. 2017;18(3) pii: E606.

Ohtsuka, M., Arase, H., Takeuchi, A., Yamasaki, S., Shiina, R., Suenaga, T. et al. **NFAM1, an immunoreceptor tyrosine-based activation motif-bearing molecule that regulates B cell development and signaling.** Proc. Natl. Acad. Sci. 2004;101(21):8126–31

de Oliveira, S., Rosowski, E.E., Huttenlocher, A. **Neutrophil migration in infection and wound repair: going forward in reverse.** Nat. Rev. Immunol. 2016;16(6):378–91

Palma, A.S., Feizi, T., Zhang, Y., Stoll, M.S., Lawson, A.M., Díaz-Rodríguez, E. et al. **Ligands for the β-glucan receptor, dectin-1, assigned using "designer" microarrays of oligosaccharide probes (neoglycolipids) generated from**

glucan polysaccharides. J. Biol. Chem. 2006;281(9):5771–9

Papayannopoulos, V., Metzler, K.D., Hakkim, A., Zychlinsky, A. **Neutrophil elastase and myeloperoxidase regulate the formation of neutrophil extracellular traps.** J. Cell Biol. 2010;191(3):677–91

Pasparakis, M., Haase, I., Nestle, F.O. **Mechanisms regulating skin immunity and inflammation.** Nat. Rev. Immunol. 2014;14(5):289–301

Saijo, S., Ikeda, S., Yamabe, K., Kakuta, S., Ishigame, H., Akitsu, A. et al. **Dectin-2 recognition of alpha-mannans and induction of Th17 cell differentiation is essential for host defense against *Candida albicans*.** Immunity. 2010;32(5):681–91

Saijo, S., Iwakura, Y. **Dectin-1 and Dectin-2 in innate immunity against fungi.** Int. Immunol. 2011;23(8):467–72

Sato, K., Yang, X., Yudate, T., Chung, J-S., Wu, J., Luby-Phelps, K. et al. **Dectin-2 is a pattern recognition receptor for fungi that couples with the Fc receptor gamma chain to induce innate immune responses.** J. Biol. Chem. 2006;281(50):38854–66

Tanno, H., Kawakami, K., Kanno, E., Suzuki, A., Takagi, N., Yamamoto, H. et al. **Invariant NKT cells promote skin wound healing by preventing a prolonged neutrophilic**

inflammatory response. Wound Repair Regen. 2017;25(5):805–15

Taylor, P.R., Reid, D.M., Heinsbroek, S.E.M., Brown, G.D., Gordon, S., Wong, S.Y.C. **Dectin-2 is predominantly myeloid restricted and exhibits unique activation-dependent expression on maturing inflammatory monocytes elicited in vivo.** Eur. J. Immunol. 2005;35(7):2163–74

Taylor, P.R., Tsoni, S.V., Willment, J.A., Dennehy, K.M., Rosas, M., Findon, H. et al. **Dectin-1 is required for beta-glucan recognition and control of fungal infection.** Nat. Immunol. 2007;8(1):31–8

Thiagarajan, P.S., Yakubenko, V.P., Elsori, D.H., Yadav, S.P., Willard, B., Tan, C.D. et al. **Vimentin is an endogenous ligand for the pattern recognition receptor Dectin-1.** Cardiovasc. Res. 2013;99(3):494–504

Thomas, G.M., Carbo, C., Curtis, B.R., Martinod, K., Mazo, I.B., Schatzberg, D. et al. **Extracellular DNA traps are associated with the pathogenesis of TRALI in humans and mice.** Blood. 2012;119(26):6335–43

Urban, C.F., Ermert, D., Schmid, M., Abu-Abed, U., Goosmann, C., Nacken, W. et al. **Neutrophil extracellular traps contain calprotectin, a cytosolic protein complex involved in host defense against Candida albicans.** PLoS Pathog. 2009;5(10) Available from:

https://www.ncbi.nlm.nih.gov/pmc/articles/PMC2763347/

Wevers, B.A., Kaptein, T.M., Zijlstra-Willems, E.M., Theelen, B., Boekhout, T., Geijtenbeek, T.B.H. et al. **Fungal engagement of the C-type lectin mincle suppresses dectin-1-induced antifungal immunity.** Cell Host Microbe. 2014;15(4):494–505

Wilgus, T.A., Roy, S., McDaniel, J.C. **Neutrophils and wound repair: Positive actions and negative reactions.** Adv. Wound Care. 2013;2(7):379–88

Wong, S.L., Demers, M., Martinod, K., Gallant, M., Wang, Y., Goldfine, A.B. et al. **Diabetes primes neutrophils to undergo NETosis, which impairs wound healing.** Nat. Med. 2015;21(7):815–9

Xu, B., deWaal, R.M., Mor-Vaknin, N., Hibbard, C., Markovitz, D.M., Kahn, M.L. **The endothelial cell-specific antibody PAL-E identifies a secreted form of vimentin in the blood vasculature.** Mol. Cell. Biol. 2004;24(20):9198–206

Yan, X., Zhang, H., Fan, Q., Hu, J., Tao, R., Chen, Q. et al. **Dectin-2 deficiency modulates Th1 differentiation and improves wound healing after myocardial infarction.** Circ. Res. 2017;120(7):1116–29

Zhu, L-L., Zhao, X-Q., Jiang, C., You, Y., Chen, X-P., Jiang, Y-Y. et al. **C-type lectin**

receptors Dectin-3 and Dectin-2 form a heterodimeric pattern-recognition receptor for host defense against fungal infection. Immunity. 2013;39(2):324–34

FIGURE LEGENDS

Figure 1. Dectin-1 and Dectin-2 levels were increased in the skin after wound creation

(a) Dectin-1 and Dectin-2 expression in the wounded tissues at the specified time points. Six wounds were created in one mouse, which were combined as one sample, and three mice were analyzed in each group. (b) Immunohistochemistry of Dectin-1, vimentin as a Dectin-1 ligand, Dectin-2, and β-glucuronidase as a Dectin-2 ligand in wounded skin at day 1 after wound creation and in unwounded skin (0 h). Arrowheads indicate Dectin-1- and Dectin-2-positive cells, respectively. Scale bar = 20 μm. (c) Flow cytometric analysis of Dectin-1- and Dectin-2-expressing cells (neutrophils, macrophages, and fibroblasts) at 24 hours after wound creation. Six wounds were created in one mouse, which were combined as one sample, and three mice were analyzed in each group. Each column represents the mean ± standard deviation. $*p < 0.05$, $**p < 0.01$

Figure 2. Effects of Dectin-1 and Dectin-2 deficiency on wound healing and neutrophil accumulation

Wounds were created on the backs of mice. (a) Representative photographs of wounds on days 0 and 5. (b) Percentage of wound closure was evaluated on day 5 (30 wounds/group). (c) Representative histological views of skin wounds are shown. Arrowheads and arrows indicate the re-epithelialized leading edges and the original wound edges, respectively. The re-epithelialization ratio on day 5 is shown (6 wounds/group). Scale bar = 500 μm. (d) The number of epithelial cells stained with PCNA antibody on day 5. Arrowheads and the dotted line indicate PCNA-positive cells and the border between epidermis and dermis, respectively.

The epithelial cell density/mm^2 was determined by counting the positive cells (5 wounds/group). Scale bar = 20 μm. (e) The number of microvessels stained with anti-CD31 antibody on day 5. Arrowheads indicate CD31-positive microvessels. The vascular density/mm^2 was determined by counting the positive vessels (5 wounds/group). Scale bar = 20 μm. (f) The number of myofibroblasts stained with α-SMA antibody on day 5. Arrowheads indicate α-SMA-positive cells. The myofibroblast density/mm^2 was determined by counting the positive cells (5 wounds/group). Scale bar = 20 μm. (g) The number of neutrophils in the wounded tissue was analyzed at 6 hours and on day 5 after wound creation. Six wounds were created in one mouse, which were combined into one sample, and five mice were analyzed in each group. Each column represents the mean ± standard deviation. *$p < 0.05$, **$p < 0.01$

Figure 3. Effects of topical administration of dZymosan or α-mannan on wound healing

Wounded WT mice received dZymosan, α-mannan, or vehicle immediately after wounding. (a) Representative photographs of wounds on days 0, 3, 5, and 7. (b) Percentage of wound closure was evaluated on days 3, 5, and 7 (30 wounds/group). (c) Representative histological views of skin wounds on day 5 are shown. Arrowheads and arrows indicate the re-epithelialized leading edges and the original wound edges, respectively. The re-epithelialization ratio on day 5 is shown (6 wounds/group). Scale bar = 500 μm. (d) Hydroxyproline content on day 5 after wound creation. Six wounds were created in one mouse, which were combined into one sample, and six mice were analyzed in each group. (e) The number of epithelial cells stained with PCNA antibody on day 5. Arrowheads and the dotted line indicate PCNA-positive cells and the border between the epidermis and dermis,

respectively. The epithelial cell density/mm^2 was determined by counting the positive cells (5 wounds/group). Scale bar = 20 μm. (f) The number of microvessels stained with anti-CD31 antibody on day 5. Arrowheads indicate CD31-positive microvessels. The vascular density/mm^2 was determined by counting the positive vessels (5 wounds/group). Scale bar = 20 μm. (g) The number of myofibroblasts stained with α-SMA antibody on day 5. Arrowheads indicate α-SMA-positive cells. The myofibroblast density/mm^2 was determined by counting the positive cells (5 wounds/group). Scale bar = 20 μm. Each column represents the mean ± standard deviation. *$p < 0.05$, **$p < 0.01$

Figure 4. Effects of topical dZymosan or α-mannan administration on the neutrophilic inflammatory responses and NETosis

Wounded WT mice received dZymosan, α-mannan, or vehicle immediately after wounding. (a) The number of neutrophils in the wounded tissue was analyzed at 6, 12, and 24 hours and on days 3, 5, and 7 after wound creation. Six wounds were created in one mouse, which were combined into one sample, and five mice were analyzed in each group. (b) TNF-α, IL-17A, CXCL1 (KC), and CXCL2 (MIP-2) levels in the wounded tissue homogenates were measured at 6 h and on day 3. The dotted line indicates the baseline of the unwounded skin. Six wounds were created in one mouse, which were combined into one sample, and five mice were analyzed in each group. (c) NET formation at the wound sites of vehicle-, dZymosan- and α-mannan-treated mice, evaluated on day 5 by immunofluorescence staining of Ly6G and Cit H3. Scale bars = 16 μm

(d) Cit H3, H3, and GAPDH expression was analyzed by Western blotting. Six wounds were created in one mouse, which were combined into one sample, and three mice were analyzed in each group. (e) Quantification levels of Cit H3 compared to histone H3 were evaluated by Western blotting analysis on day 5. (f) Quantification levels of Cit H3 compared to histone H3 were evaluated using Western blotting analysis at 6 h. Six wounds were created in one mouse, which were combined into one sample, and three mice were analyzed in each group. Each column represents the mean ± standard deviation. $*p < 0.05$, $**p < 0.01$

Figure 5. Effect of Dectin-1 and Dectin-2 deficiency, DNase, and neutrophil depletion on NET formation

(a) NET formation at wound sites of wounded WT mice that did not receive any treatment at each of the specified time points. Cit H3, H3, and GAPDH expression was analyzed by Western blotting (left). Quantification levels of Cit H3 compared to histone H3 were evaluated using Western blotting (right). Six wounds were created in one mouse, which were combined into one sample, and three mice were analyzed in each group. (b) Quantification levels of Cit H3 compared to histone H3 at the wound sites of WT mice and Dectin-2KO mice were evaluated on day 3. Six wounds were created in one mouse, which were combined into one sample, and three mice were analyzed in each group. (c) Quantification levels of Cit H3 compared to histone H3 at the wound sites of WT mice and Dectin-1KO mice were evaluated on day 3. Six wounds were created in one mouse, which were combined into one sample, and three mice were analyzed in each group. (d) WT mice were injected

intraperitoneally with DNase or vehicle from 1 day before wounding to 1 day before tissue collection. Wounded WT mice received α-mannan or vehicle immediately after wounding. The percentage of wound closure was evaluated on day 5 (18 wounds/group). (e) The percentage of wound closure was evaluated on day 3 (18 wounds/group). (f) Quantification levels of Cit H3 compared to histone H3 at the wound sites were evaluated on day 5. Six wounds were created in one mouse, which were combined into one sample, and three mice were analyzed in each group. (g) Wounds were created on the backs of mice and anti-Gr-1 monoclonal antibody or control IgG was injected intraperitoneally 1 day after wounding. The percentage of wound closure was evaluated on day 3 (18 wounds/group). (h) Quantification levels of Cit H3 compared to histone H3 at the wound sites were evaluated on day 3. Six wounds were created in one mouse, which were combined into one sample, and three mice were analyzed in each group. Each column represents the mean ± standard deviation. *$p <$ 0.05, **$p < 0.01$

Figure 6. Effect of Dectin-2 deficiency on wound maturation

Wounds were created on the backs of Dectin-2-KO or WT mice. (a) Hydroxyproline content in the wounded tissue was evaluated on day 10. Six wounds were created in one mouse, which were combined into one sample, and six mice were analyzed in each group. (b) The COL3A1-to-COL1A1 ratio in wounded tissues was evaluated on day 10. Six wounds were created in one mouse, which were combined into one sample, and six mice were analyzed in each group. (c) TGF-β1 expression was evaluated on day 5. Six wounds were created in one mouse, which were combined into one sample, and six mice were analyzed in each group. (d)

MMP-2 and MMP-8 expression was evaluated on day 10. Six wounds were created in one mouse, which were combined into one sample, and six mice were analyzed in each group. (e) Neutrophil elastase activity in the homogenized wound tissue was evaluated on day 3. Six wounds were created in one mouse, which were combined into one sample, and five mice were analyzed in each group. Each column represents the mean ± standard deviation. *$p < 0.05$, **$p < 0.01$

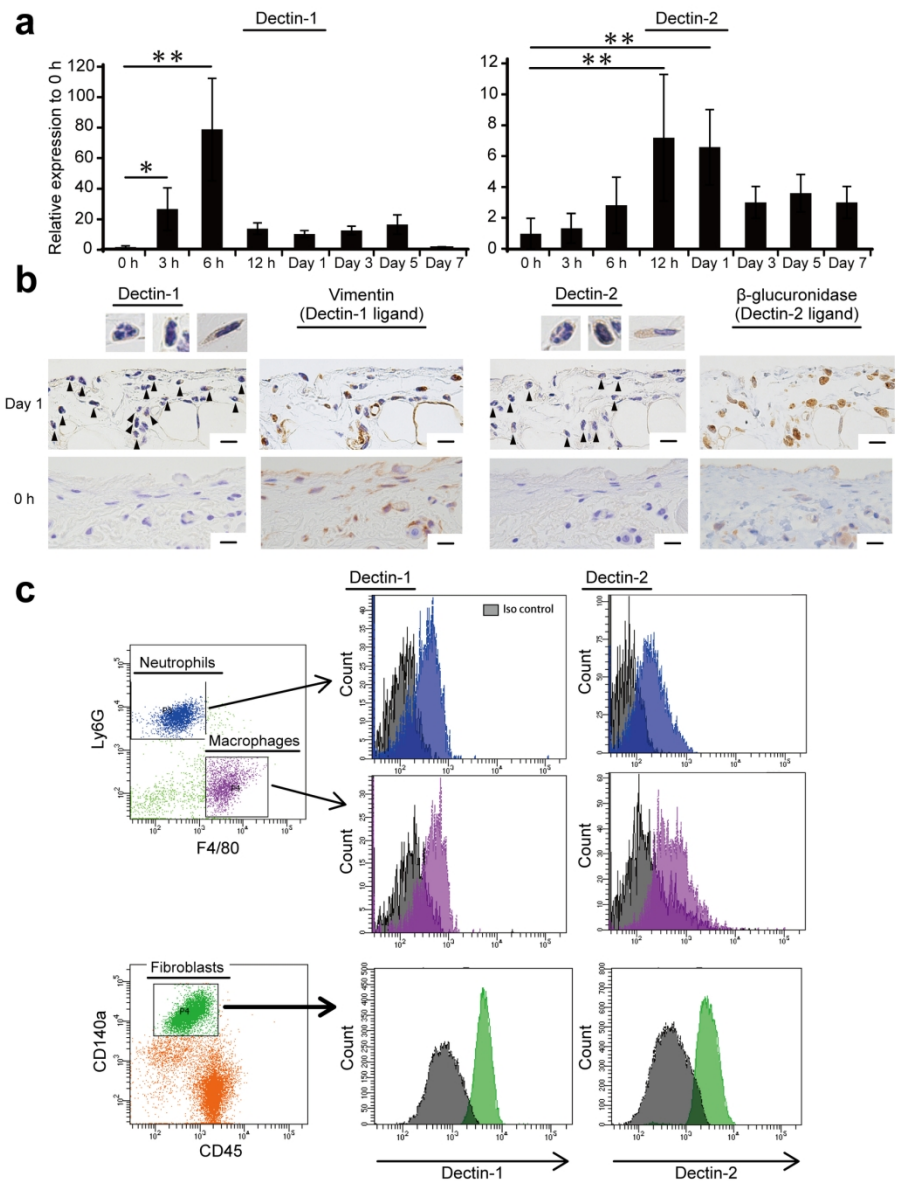

150x199mm (300 x 300 DPI)

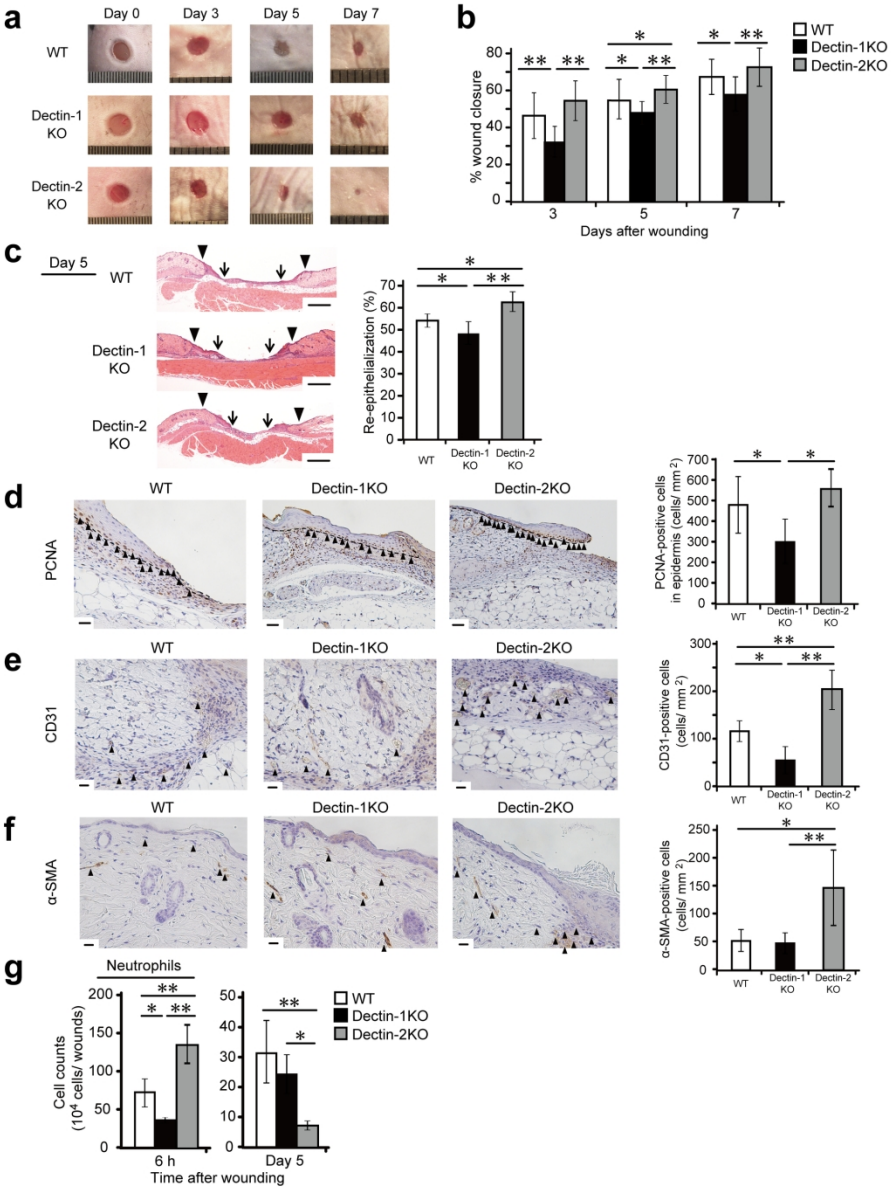

175x228mm (300 x 300 DPI)

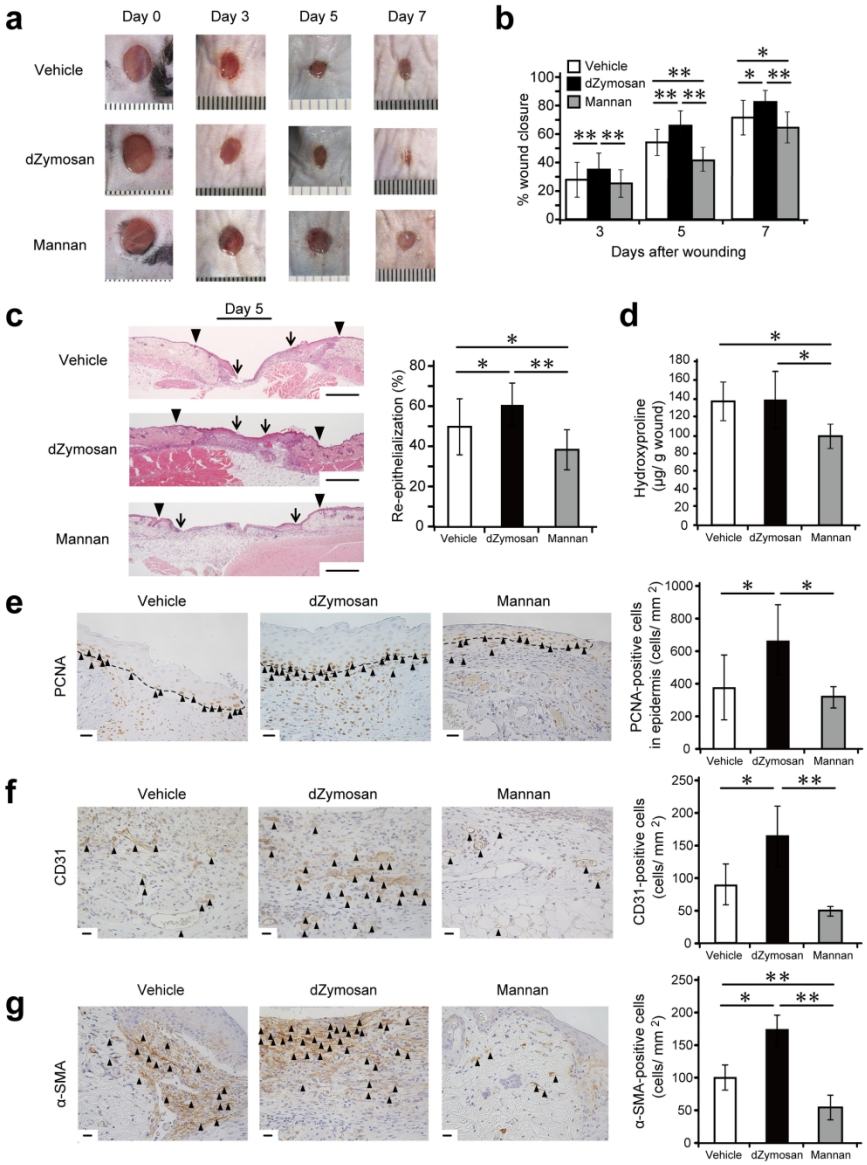

175x228mm (300 x 300 DPI)

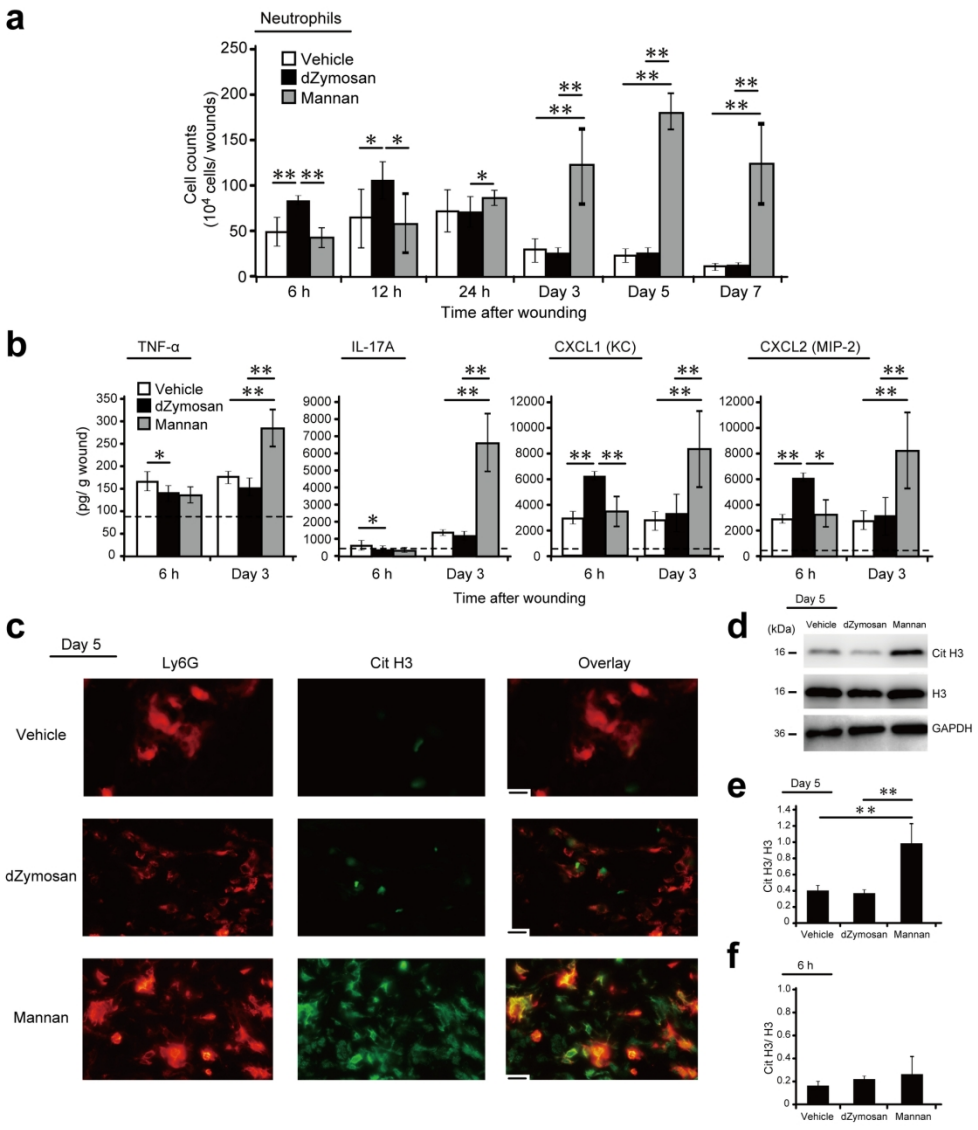

175x199mm (300 x 300 DPI)

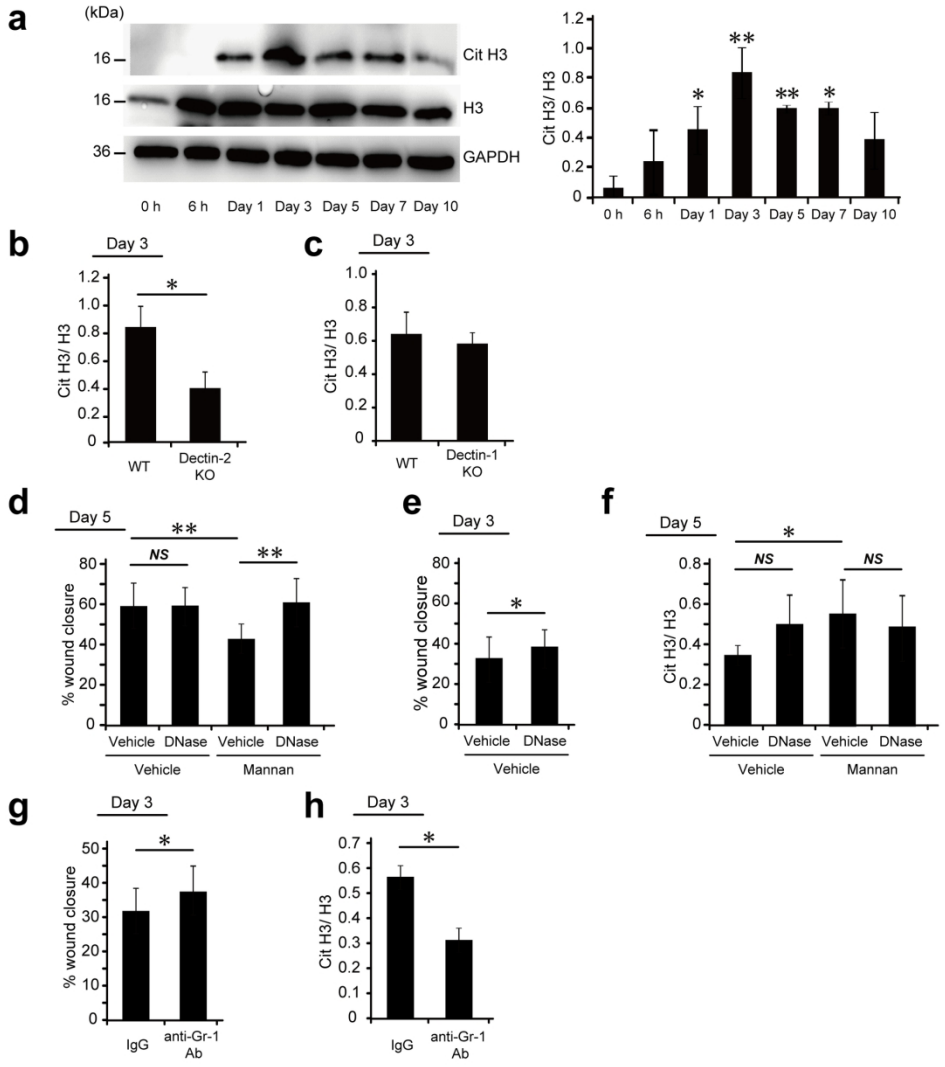

175x192mm (300 x 300 DPI)

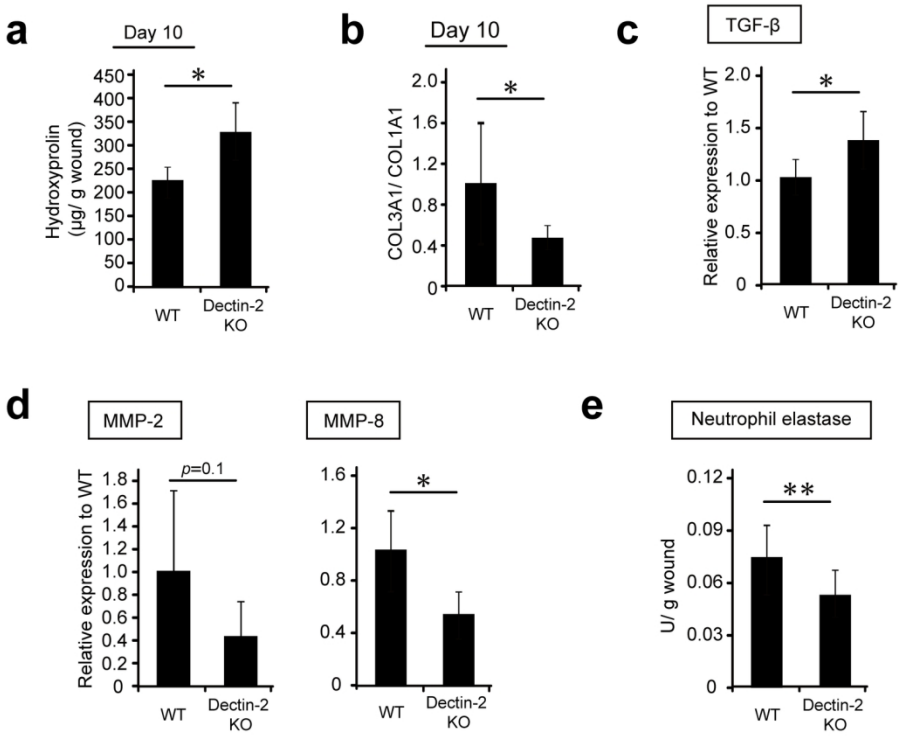

150x122mm (300 x 300 DPI)

SUPPLEMENTARY MATERIALS AND METHODS

Mice

Dectin-1 KO mice were generated by homologous recombination of the Clec7a gene as described previously (Saijo and Iwakura, 2011) and backcrossed to C57BL/6 mice for eight generations. Dectin-2 gene-disrupted (knockout [KO]) mice were generated by homologous recombination of the Clec4n gene as described previously (Saijo et al., 2010) and backcrossed to C57BL/6 mice for seven generations or for more than eight generations. CARD9 KO mice were generated and established as described previously (Hara et al., 2007) and backcrossed to C57BL/6 mice for more than eight generations. Wild-type (WT) littermate mice of Dectin-2KO mice were used as controls for seven generations. Except for experiments with Dectin-2KO mice that were established over seven generations, C57BL/6 mice purchased from CLEA Japan (Tokyo, Japan) were used as WT control. Male mice at 7 to 10 weeks of age were used in the experiments. Food and water were available *ad libitum*. All mice were kept under specific pathogen-free conditions in the Institute for Animal Experimentation, Tohoku University Graduate School of Medicine (Sendai, Japan).

Wound creation and tissue collection

All wound creation was performed under anesthesia that was induced by an intraperitoneal injection of 40 mg/kg sodium pentobarbital (Somnopentyl, Kyoritsu Seiyaku Corporation, Tokyo, Japan), and sustained by inhalation anesthesia of isoflurane (Isoflurane, Mairan Pharma, Osaka, Japan). The dorsal hair was shaved to fully expose the skin, which was then rinsed with 70% ethanol. Six full-thickness wounds extending to the panniculus carnosus

were created on each mouse using a 3-mm diameter biopsy punch (Biopsy Punch, Kai Industries Co., Ltd., Gifu, Japan) under sterile conditions. The wounds were covered with a polyurethane film (Tegaderm Transparent Dressing, 3M Health Care, St. Paul, MN, USA) and an elastic adhesive bandage (Hilate, Iwatsuki, Tokyo, Japan) as an occlusive dressing. The day on which the wounds were made was day 0. At various time points, mice were sacrificed and wound tissue was collected by excising the tissue using an 8-mm diameter biopsy punch.

Treatment with dZymosan (zymosan depleted) or α-mannan

dZymosan (zymosan depleted), which was prepared from *Saccharomyces cerevisiae* cell walls treated with hot alkali to remove all their TLR-stimulating properties, was purchased from Invivogen (San Diego, CA, USA) and diluted with phosphate buffered saline (PBS) at 0.5 mg/mL. Mannan from *Saccharomyces cerevisiae* (α-mannan) was purchased from Sigma-Aldrich (St. Louis, MO, USA) and diluted with phosphate buffered saline (PBS) at 10 mg/mL. Wounds were created in accordance with the method described above, and immediately after wounding, a 3-μL suspension of dZymosan (2.5 μg), α-mannan (30 μg), or PBS as a vehicle control was applied to the base of the wounds in WT, Dectin-1KO, or Dectin-2KO mice.

Administration of deoxyribonuclease (DNase) I

DNase I, a deoxyribonuclease for single-stranded DNA and double-stranded DNA, was purchased from FUJIFILM Wako Pure Chemical Co. (Osaka, Japan) and dissolved in normal saline at a concentration of 250 U/mL. To inhibit single- and double-stranded DNA, WT mice

and WT mice treated with α-mannan were injected intraperitoneally with a 200 μL suspension of DNase I (50 U) each day from 1 day before wounding to 1 day before tissue collection. As a control group for the relevant experiments, mice were injected with normal saline at the same time points.

Neutrophil depletion with anti-Gr-1 antibody

Anti-Gr-1 monoclonal antibody was purified from hybridoma culture supernatants (clones RB6-8C5) using a protein G column kit (Kirkegaard & Perry Laboratories, Gaithersburg, MD, USA). This monoclonal antibody (Gr-1) completely depletes mouse neutrophils (Miura et al., 2019). To neutralize the biological activity of neutrophils, mice were injected intraperitoneally with 400 μg of mAb at 24 hours after wounding. Rat IgG (ICN Pharmaceuticals, Aurora, OH, USA) was used as a control antibody.

Measurement of wound areas

Wound areas were measured on digital images that were obtained with a digital camera (CX4; Ricoh, Tokyo, Japan). After the wounds were created, photographs were taken of each wound before dressing. At various time points, the polyurethane films were removed from the mice and the wounds were photographed. Each wounded area was quantified by tracing its margin and calculating the pixel area using AxioVision imaging software, release 4.6 (Carl Zeiss Micro Imaging Japan, Tokyo, Japan). The percentage of wound closure was calculated using the following formula: % wound closure = (1 – wound area at the indicated time point / wound area 1 on day 0) × 100.

Analysis of hydroxyproline content

Wounds were removed using an 8-mm diameter biopsy punch after mice were sacrificed, and total wound hydroxyproline content was assayed. Briefly, all wound tissue was homogenized and then hydrolyzed in 6N HCl for 21 hours at 120°C. The hydrolysate was neutralized with NaOH. In the next step, 2-mL aliquots were analyzed calorimetrically for hydroxyproline content adding 1 mL of 0.05 mol/L chloramine T (Nacalai Tesque, Kyoto, Japan), 1 mL of 3.15 mol/L perchloric acid (Nacalai Tesque), and 1 mL of 20% dimethylaminobenzaldehyde (Nacalai Tesque). The optical densities of the samples were determined using a spectrophotometer at 557 nm.

Histology and immunohistochemistry

The removed wound tissues were fixed with 4% paraformaldehyde-phosphate buffer solution and embedded in paraffin. Sections were taken from the central portion of the wound and stained with hematoxylin-eosin (HE) in accordance with the standard method. The extent of re-epithelialization in each wound was measured in these HE-stained sections by measuring the distance from the normal wound margin to the edge of the epithelium. The re-epithelialization index was determined based on the percentage of new epithelium that was present in the total wound.

For immunohistochemistry, after blocking with endogenous peroxidase using methanol/ hydrogen peroxide, the sections were incubated with 10% normal rabbit serum for 20 min to block non-specific binding and then stained with anti-Dectin-1 Ab (dilution 1:25;

BioLegend, San Diego, CA, USA), anti-Dectin-2 Ab (dilution 1:100; Bio-Rad Laboratories, Hercules, CA, USA), anti-Vimentin Ab (dilution 1:100; Abcam plc, Cambridge, UK), anti-β-glucuronidase (dilution 1:100; Proteintech, Rosemont, IL, USA), anti-proliferating cell nuclear antigen (PCNA) Ab (dilution 1:100; Agilent Technologies, Santa Clara, CA, USA), anti-α-smooth muscle actin (α-SMA) Ab (dilution 1:300; Vector Laboratories, Inc., Burlingame, CA, USA), and anti-CD31 (PECAM-1) Ab (0.25 μg/mL; Santa Cruz Biotechnology, Santa Cruz, CA, USA). The sections were incubated with peroxidase-conjugated secondary Ab (4 μg/mL; Histofine Simple Stain MAX-PO, Nichirei Bioscience, Tokyo, Japan).

Epithelial cell differentiation, vascular density in the granulation tissue, and myofibroblast differentiation were determined by counting the number of PCNA-positive epithelial cells, the number of CD31-positive vessels, and the number of α-SMA-positive cells, respectively. All analyses were performed under blinded conditions.

For fluorescent immunostaining, the tissues were embedded in OCT compound (Sakura Finetechnical Co., Tokyo, Japan) and quickly frozen. The sections were taken from the central portion of the wound, blocked with 10% normal goat serum (Nichirei Bioscience, Tokyo, Japan), and incubated with a primary Ab against citrullinated histone H3 (Cit H3) (rabbit) (0.04 μg/mL; Abcam) and anti-Ly6G (rat) (clone 1A8, 5 μg/mL; BioLegend) at 4°C overnight, and then with Alexa 488-conjugated secondary Ab (anti-rabbit) (0.02 μg/mL; Life Technologies, Tokyo, Japan) and Alexa 555-conjugated secondary Ab (anti-rat) (0.02 μg/mL; Life Technologies) for 30 min at room temperature (RT). After the sections were covered with mountant (VECTASHIELD® Hard Set Mounting Medium; Vector Laboratories, Inc.), images

were acquired by fluorescence microscopy (FSX100; Olympus, Tokyo, Japan).

Preparation of leukocytes in the wound tissue

Mice were sacrificed at 6, 12, or 24 hours or on days 3, 5, or 7 after wound creation. The wound tissues were excised using a biopsy punch (8 mm in diameter) and teased apart using stainless-steel mesh in RPMI 1640 medium (Nipro, Osaka, Japan) supplemented with 10 mM HEPES, 10% fetal calf serum (FCS) (BioWest, Nuaillé, France), 1 mg/mL collagenase, and 1 mg/mL hyaluronidase (Sigma-Aldrich). They were incubated for 2 hours at 37°C with vigorous shaking. After incubation, the tissue fragments and most dead cells were removed by passing the cells through a 70-μm cell strainer (BD Falcon, Bedford, MA, USA). They were then washed three times with 1% FCS RPMI 1640 medium and used as skin leukocytes for flow cytometric analysis.

Analysis of Dectin-1, 2-positive cells using flow cytometry

The cells obtained from the wound tissues were stained with Pacific blue-anti-CD45 monoclonal antibody (mAb) (clone 30-F11, BioLegend), allophycocyanin cyanin 7 (APC/Cy7)-anti-Ly6G mAb (clone 1A8, BioLegend), phycoerythrin (PE)-anti-F4/80 mAb (clone BM8, BioLegend), allophycocyanin (APC)-anti-CD140a mAb (clone APA5, BioLegend), APC-anti-Dectin-1 mAb (clone RH1, BioLegend), and fluorescein isothiocyanate (FITC)-anti-Dectin-2 mAb (clone KVa7-6E7, Miltenyi Biotec, Bergisch Gladbach, Germany). Isotype-matched irrelevant IgG was used as the control staining. Macrophages and neutrophils were identified as CD45+F4/80+ cells and CD45+Ly6G+ cells,

respectively. Fibroblasts were identified as CD45+CD140a+ cells. The stained cells were analyzed using a BD FACS Canto II flow cytometer (BD Bioscience, San Jose, CA, USA).

Analysis of leukocyte fraction using flow cytometry

The cells obtained from wounded tissues were stained with Pacific blue-anti-CD45 mAb (clone 30-F11, BioLegend), APC-anti-CD11b mAb (clone M1/70, BioLegend), APC/Cy7-anti-Ly6G mAb (clone 1A8, BioLegend), and Alexa Fluor®488-anti-F4/80 mAb (clone BM8, BioLegend). Isotype-matched irrelevant IgG was used for control staining. Macrophages and neutrophils were identified as CD45+CD11b+F4/80+ cells and CD45+CD11b+Ly6G+ cells, respectively. The stained cells were analyzed using a BD FACS Canto II flow cytometer (BD Bioscience). The numbers of neutrophils and macrophages were estimated by multiplying the total leukocyte number by the proportion of each fraction.

RNA extraction and quantitative real-time RT-PCR

Total RNA was extracted from wound tissues using ISOGEN (Nippon Gene Co. Ltd., Tokyo, Japan), and first-strand cDNA was synthesized using a PrimeScript first-strand cDNA synthesis kit (TaKaRa Bio Inc., Otsu, Japan), in accordance with the manufacturer's instructions. Quantitative real-time polymerase chain reaction (PCR) was performed in a volume of 20 μL using gene-specific primers and FastStart essential DNA green master mix (Roche Applied Science, Branford, CT, USA) in a Step One™ (Thermo Fisher, Waltham, MA, USA). Primers were as follows: 5′-CCTTGGAGGCCCATTGC-3′ (Forward) and 5′-GCAACCACTACTACCACAAAGCA-3′ (Reverse) for Dectin-1; 5′-CTG GAG CAC CAG

TGA GCA GAA C-3′ (Forward), and 5′-CCA TTT GCC ATT ACC TTG TGG A-3′ (Reverse) for Dectin-2; 5′-AAG ACA AGG CAG CGG TGG AA-3′ (Forward) and 5′- GCA GGG GAC AGG AAA TAG TT-3′ (Reverse) for COL1A1; 5′-GGA CCA GGC AAT GAT GGA AAA CC-3′ (Forward) and 5′-ACC AGG GAA ACC CAT GAC ACC-3′ (Reverse) for COL3A1; 5′-TAC GCC TGA GTG GCT GTC TTT T-3′ (Forward) and 5′-CGT GGA GTT TGT TAT CTT TGC TGT-3′ (Reverse) for TGF-β; 5′-CCC CTG ATG TCC AGC AAG TAG A-3′ (Forward) and 5′-AGT CTG CGA TGA GCT TAG GGA AA-3′ (Reverse) for MMP-2; 5′-GAT TCA GAA ACG TGG ACT CAA-3′ (Forward) and 5′-CAT CAA GGC ACC AGG ATC AGT-3′ (Reverse) for MMP-8; and 5′-GCT TCC TCA GAC CGC TT-3′ (Forward) and 5′-TCG CTA ATC ACG CTG GG-3′ (Reverse) for β-actin (ACTB). The reaction efficiency with each primer set was determined using standard amplifications. Target gene expression levels and that of ACTB as a reference gene were calculated for each sample using the reaction efficiency. The results were analyzed using a relative quantification procedure and are presented as expression levels relative to ACTB expression.

Measurement of cytokine concentrations

The wound tissues were homogenated with saline solution, and the concentrations of cytokine and chemokine in the supernatants were measured using appropriate enzyme-linked immunosorbent assay (ELISA) kits (BioLegend for TNF-α and IL-17A; R&D Systems for CXCL1, CXCL2, and CCL2). The results were expressed as the values per wound.

Western blot analysis

Frozen skin wound tissues were weighed and homogenized in RIPA buffer (Wako Pure Chemical Industries, Osaka, Japan) supplemented with Protease Inhibitor Cocktail (Sigma-Aldrich) on ice. After centrifugation at 20,000 ×*g* for 20 min at 4°C, the protein concentration was determined using the bicinchoninic acid method (Pierce Biotechnology, Rockford, IL, USA). An equal amount of protein per sample was separated by SDS-PAGE using gradient gels (4–20% Tris-Glycine gels, Bio-Rad Laboratories) and transferred to polyvinylidene difluoride membranes (ATTO Corporation, Tokyo, Japan) using a semidry transblot system (ATTO Corporation). Non-specific binding on the blots was blocked with 0.5% (w/v) skim milk and 0.1% (v/v) Tween 20 in TBS for 2 hours at RT, followed by incubation for 1 hour at RT with primary antibodies (rabbit polyclonal anti-Cit H3, 1:1000, Abcam; rabbit polyclonal anti-H3, 1:2000, cell signaling; mouse anti-GAPDH, 1:2000, MBL, Nagoya, Japan) overnight at 4°C. Blots were incubated with appropriate HRP-conjugated secondary antibodies (goat anti-rabbit IgG, 1:5000, cell signaling; goat anti-mouse IgG, 1:5000, cell signaling) for 1 hour at RT. The blots were developed with enhanced chemiluminescence substrate (Nacalai Tesque, cat. no. 11644). Chemiluminescent signals were detected using ImageQuant LAS 4000 analyzer (FujiFilm, Tokyo, Japan). Blots were quantified using ImageJ software.

Measurement of neutrophil elastase activity

The wound tissue was homogenized with PBS, and the concentration of elastase activity was measured using the EnzChek Elastase Assay Kit (Thermo Fisher), in accordance with the manufacturer's instructions. The results were expressed as the values per wound. The detection limit was 0.004 U/mL.

Preparation of skin supernatant using wounded tissues and Dectin-1- and Dectin-2-NFAT–GFP reporter assay

Mice were sacrificed at 24 hours after wound creation. The wounded tissues were excised using a biopsy punch (8 mm in diameter) and the tissue from six wounds was homogenized in 2 mL of RPMI 1640 medium using stainless-steel mesh. After homogenization, most dead cells were removed by passing the cells through an 8-μm cell strainer (BD Falcon).

T cell hybridoma 2B4 cells were transfected with the NFAT-GFP construct prepared by fusing three tandem NFAT-binding sites with enhanced GFP cDNA (Ohtsuka et al., 2004). This cell line was transfected with Dectin-1 or Dectin-2 and FcRγ genes, and the same cell line lacking Dectin-1 or Dectin-2 was used as a control. These cells were stimulated with the above-mentioned skin supernatant or 60 μg/mL dZymosan for Dectin-1 reporter cells, or 3 mg/mL α-mannan for Dectin-2 reporter cells as a positive control, for 20 hours. Additionally, 10% FCS RPMI 1640 medium was used as a control medium. After the stimulation, these cells were stained with allophycocyanin (APC)-anti-CD3 mAb. GFP expression was analyzed in the CD3+ cells but not in the dead 7-aminoactinomycin D (7-AAD)-stained cells by flow cytometry.

Statistics

Data are expressed as the mean ± standard deviation (SD). Data analysis was performed using Welch's *t*-test to compare two experimental groups, and a one-way ANOVA with post-hoc Dunnett's or Turkey–Kramer's honestly significant difference (HSD) test was used for more

than three experimental groups. A p value less than 0.05 was considered to indicate significance.

Study approval

All experimental protocols described in the present study were approved by the Ethics Review Committee for Animal Experimentation of Tohoku University and performed in accordance with institutional ethical guidelines.

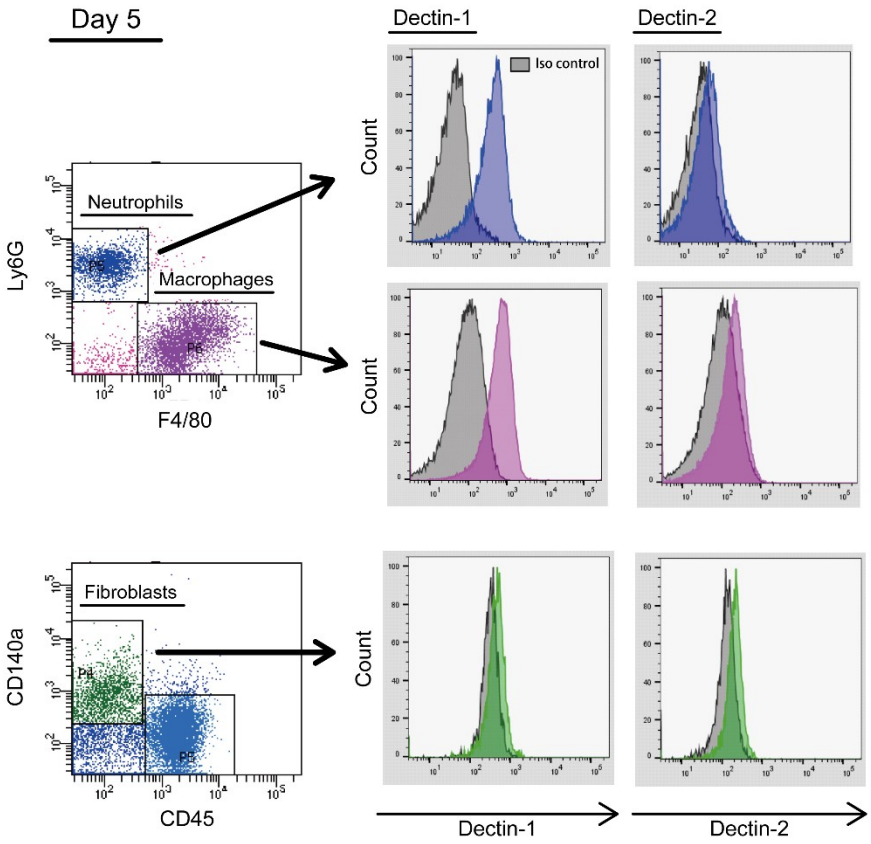

Supplementary Figure S1. Dectin-1 and Dectin-2 expression in the wounded tissues at day 5
Flow cytometric analysis of Dectin-1 and Dectin-2-expressing cells (neutrophils, macrophages, and fibroblasts) at day 5 after wound creation.

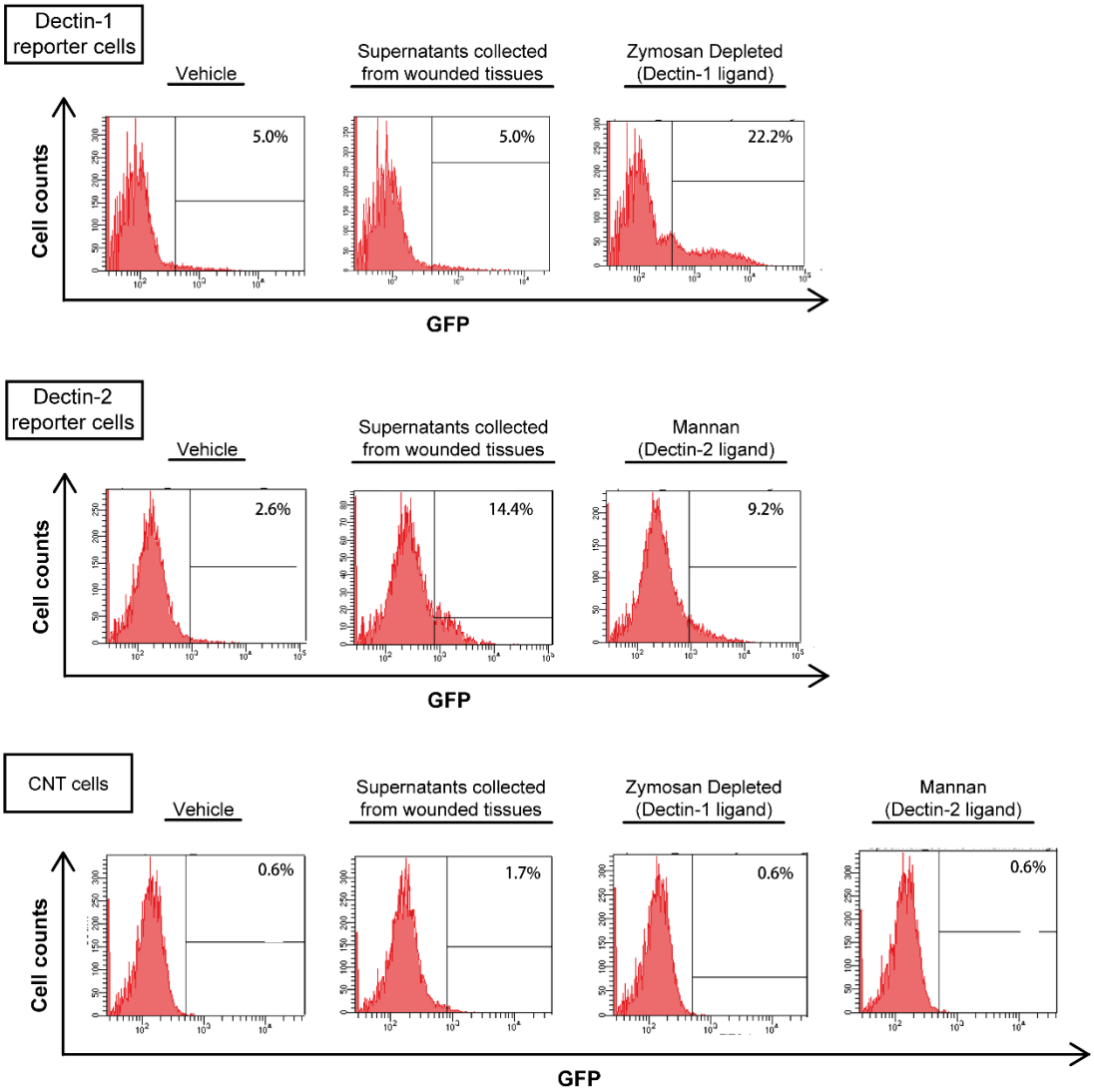

Supplementary Figure S2. Dectin-1 and Dectin-2-NFAT-GFP reporter assay
The NFAT-GFP reporter cells expressing Dectin-1 or Dectin-2 were cultured with supernatants that were collected from the wounded tissues 24 hours after wound creation, and GFP expression was analyzed using flow cytometry. Vehicle, dZymosan, and α-mannan were used as controls. Reporter cells expressing FcRγ alone were used as control (CNT) cells.

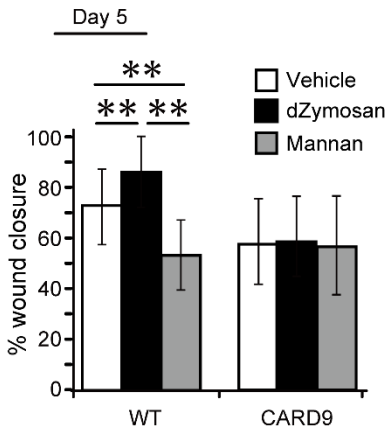

Supplementary Figure S3. Involvement of CARD9 in the effects of topical administration of dZymosan or α-mannan

CARD9 is an essential signaling adaptor molecule via CLRs. Wounded WT or CARD9KO mice received dZymosan, α-mannan, or vehicle immediately after wounding. The percent of wound closure was evaluated on day 5 (n=18 wounds/group). Each column represents the mean ± standard deviation. *$p < 0.05$, **$p < 0.01$

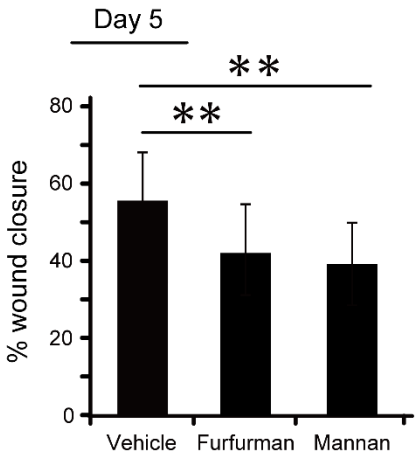

Supplementary Figure S4. Topical administration of Furfurman (another Dectin-2 ligand) leads to delayed wound closure. Furfurman is derived from *Malassezia furfur* cell walls. Wounded WT mice received Furfurman, vehicle, or mannan immediately after wounding. The percent of wound closure was evaluated on day 5 (n=18 wounds/group). Each column represents the mean ± standard deviation. *$p <$ 0.05

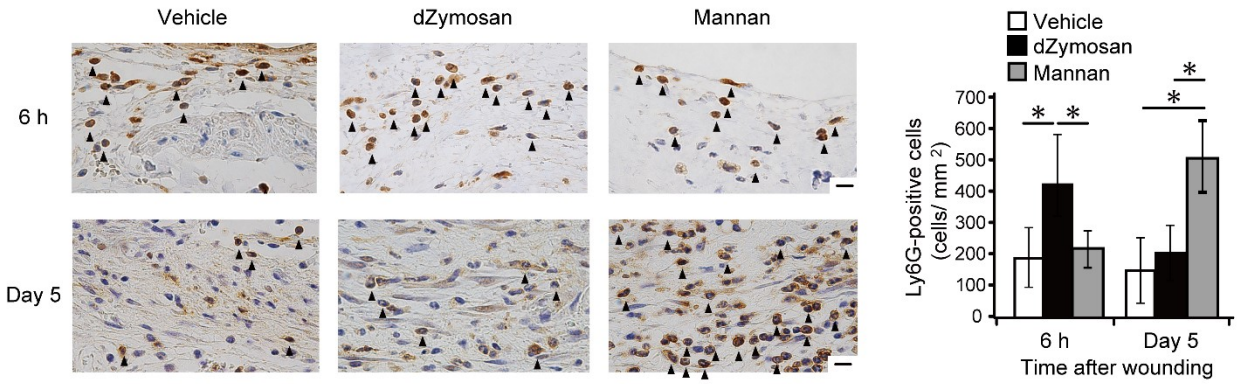

Supplementary Figure S5. Effects of dZymosan or α-mannan topical administration on neutrophil accumulation

Wounded WT mice received dZymosan, α-mannan, or vehicle immediately after wounding. The number of neutrophils that were stained with Ly6G antibody was analyzed at 6 hours and on day 5. Arrowheads indicate Ly6G-positive neutrophils. The neutrophil density/mm^2 was determined by counting the positive cells (n = 6 wounds/group). Scale bar = 20 μm

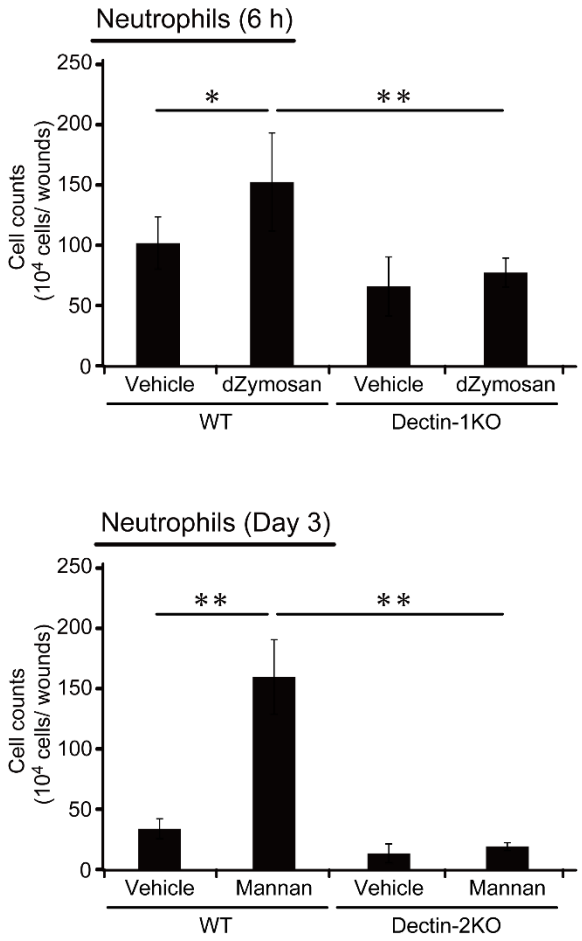

Supplementary Figure S6. Effects of topical dZymosan or α-mannan administration on the neutrophil accumulation in Dectin-1KO or Dectin-2KO

(a) Wounded Dectin-1KO or WT mice received dZymosan or vehicle immediately after wounding. The number of neutrophils in the wounded tissue was analyzed at 6 hours after wound creation. Six wounds were created in one mouse, which were combined into one sample, and five mice were analyzed in each group. (b) Wounded Dectin-2KO or WT mice received α-mannan (Mannan) or vehicle immediately after wounding. The number of neutrophils in the wounded tissue was analyzed at day 3 after wound creation. Six wounds were created in one mouse, which were put combined one sample, and five mice were analyzed in each group. Each column represents the mean ± standard deviation. *$p < 0.05$, **$p < 0.01$

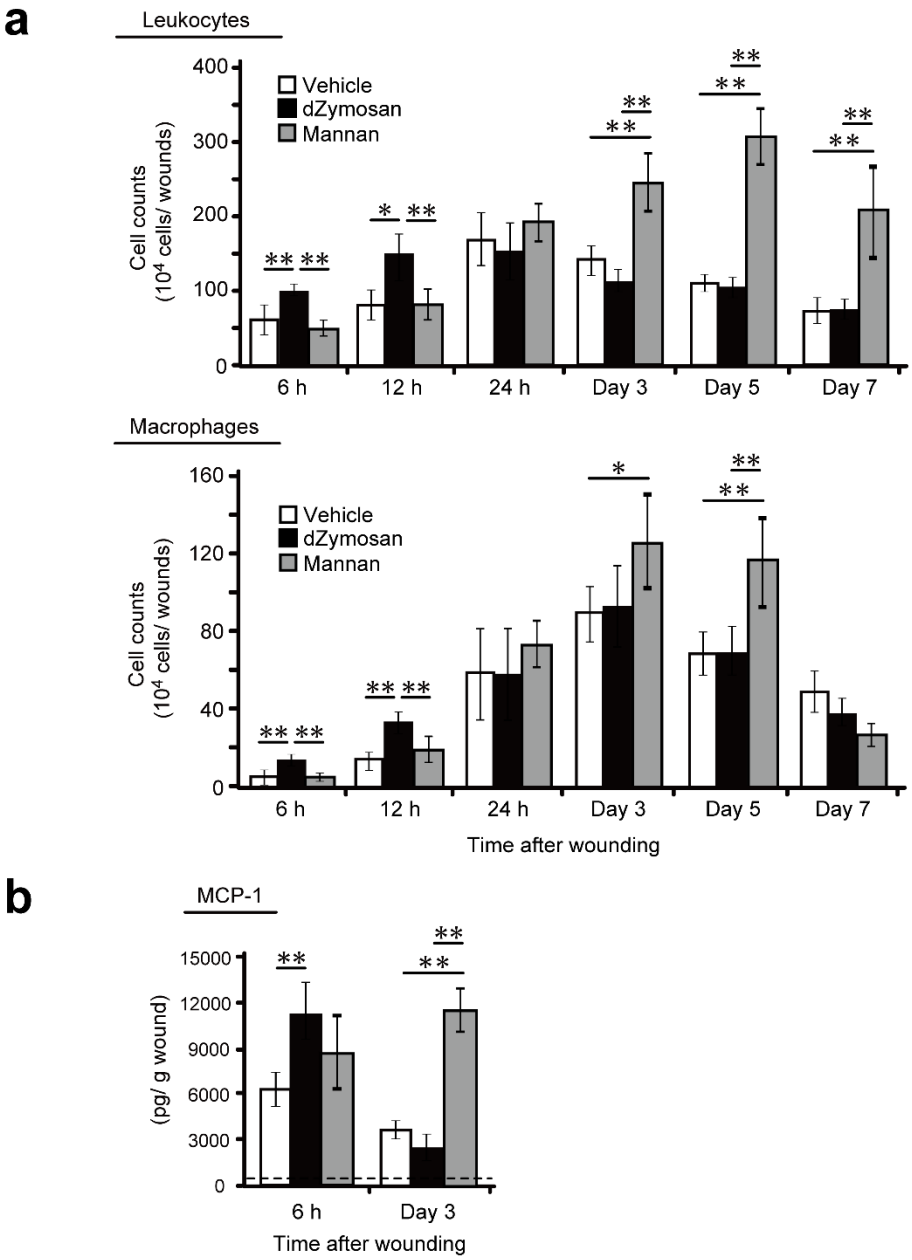

Supplementary Figure S7. Effects of topical dZymosan or α-mannan administration on leukocyte and macrophage accumulation. Wounded WT mice received dZymosan, α-mannan, or vehicle immediately after wounding. (a) The numbers of leukocytes and macrophages in the wounded tissue were analyzed by flow cytometry at 6, 12, and 24 hours and on days 3, 5, and 7 after wound creation. Six wounds were created in one mouse, which were combined into one sample, and five mice were analyzed in each group. (b) MCP-1 levels in the wounded tissue homogenates were measured at 6 hours and on day 3. Six wounds were created in one mouse, which were combined into one sample, and five mice were analyzed in each group. The dotted line indicates the baseline of un-wounded skin. Each column represents the mean ± standard deviation. *$p < 0.05$, **$p < 0.01$

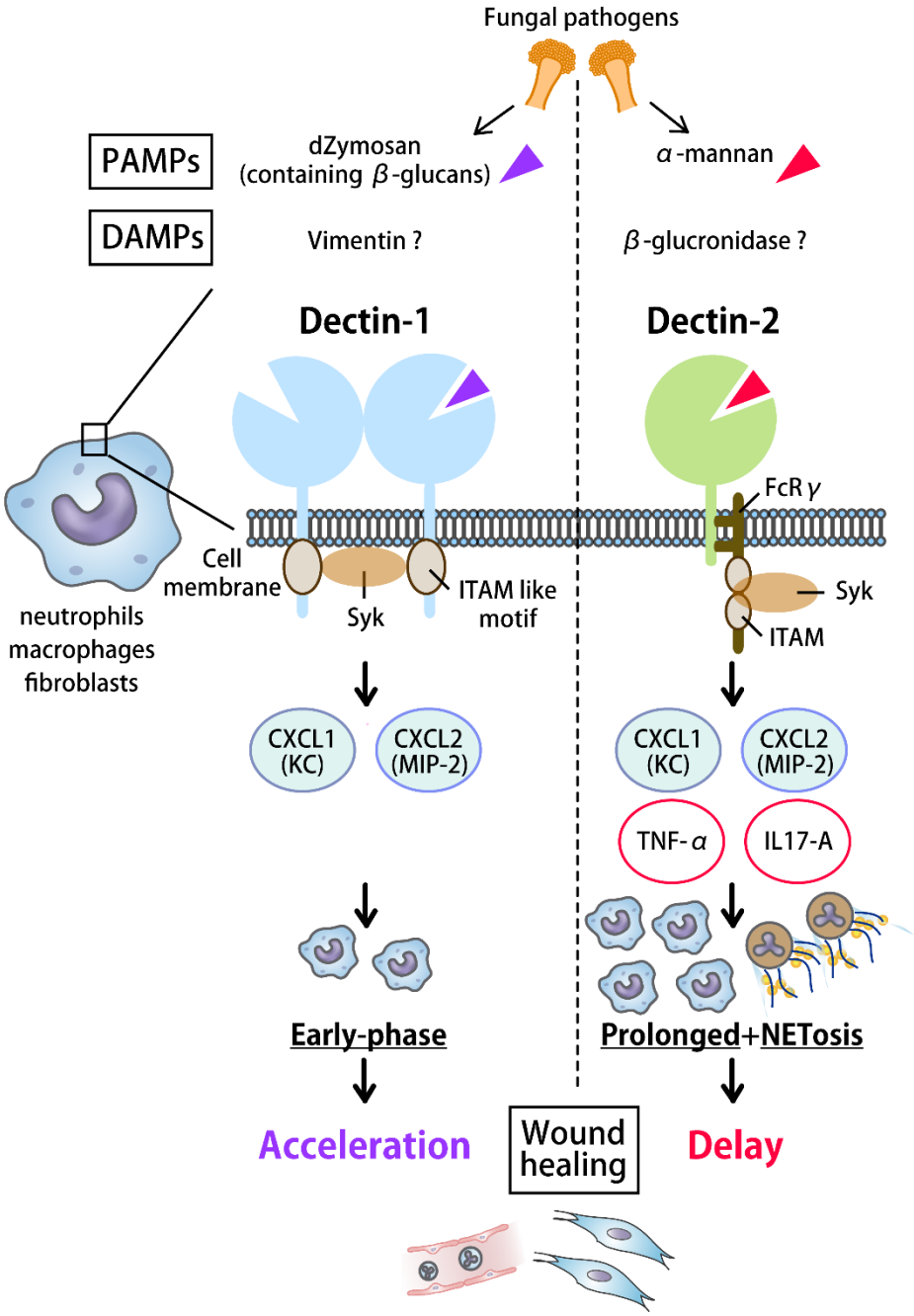

Supplementary Figure S8. Distinct roles for Dectin-1 and Dectin-2 in skin wound healing and neutrophilic inflammatory responses

Dectin-1 and Dectin-2 contribute to inflammatory responses that are triggered by β-glucan and α-mannan, which are both derived from the fungal cell wall. Additionally, vimentin and β-glucuronidase from damaged tissues may also be involved in these responses. The main findings in the current study are as follows: 1) Dectin-1 and Dectin-2 were expressed in neutrophils, macrophages, and fibroblasts at the wound sites; 2) Dectin-1 contributed to the acceleration of wound healing by inducing early phase neutrophil accumulation via KC and MIP-2 production; and 3) Dectin-2 was involved in prolonged neutrophilic responses and NET formation, leading to delayed wound healing accompanied by TNF-α and IL-17A induction.

Thus, for skin wound healing, Dectin-1 and Dectin-2 showed distinct roles through their different effects on the neutrophilic response.

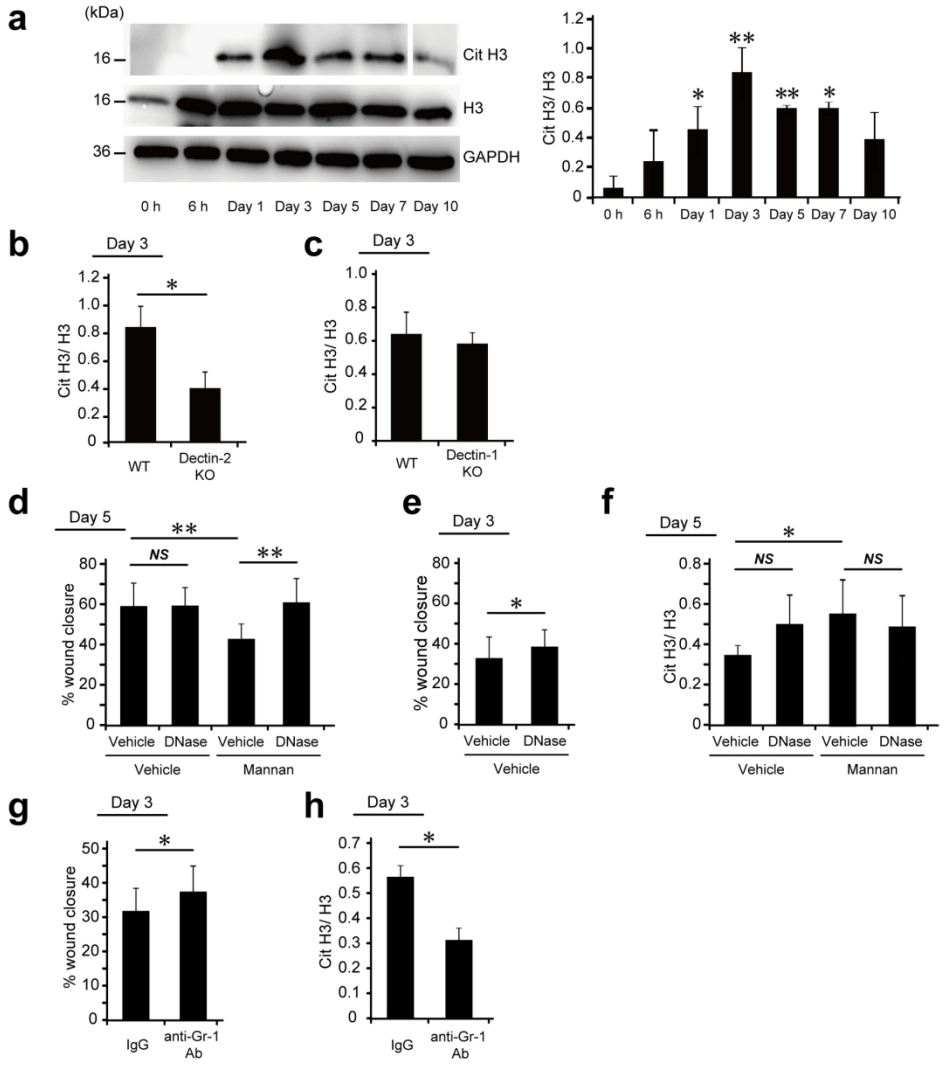

Figure 5. R1

175x192mm (300 x 300 DPI)

SUPPLEMENTARY MATERIALS AND METHODS

Mice

Dectin-1 KO mice were generated by homologous recombination of the Clec7a gene as described previously (Saijo and Iwakura, 2011) and backcrossed to C57BL/6 mice for eight generations. Dectin-2 gene-disrupted (knockout [KO]) mice were generated by homologous recombination of the Clec4n gene as described previously (Saijo et al., 2010) and backcrossed to C57BL/6 mice for seven generations or for more than eight generations. CARD9 KO mice were generated and established as described previously (Hara et al., 2007) and backcrossed to C57BL/6 mice for more than eight generations. Wild-type (WT) littermate mice of Dectin-2KO mice were used as controls for seven generations. Except for experiments with Dectin-2KO mice that were established over seven generations, C57BL/6 mice purchased from CLEA Japan (Tokyo, Japan) were used as WT control. Male mice at 7 to 10 weeks of age were used in the experiments. Food and water were available *ad libitum*. All mice were kept under specific pathogen-free conditions in the Institute for Animal Experimentation, Tohoku University Graduate School of Medicine (Sendai, Japan).

Wound creation and tissue collection

All wound creation was performed under anesthesia that was induced by an intraperitoneal injection of 40 mg/kg sodium pentobarbital (Somnopentyl, Kyoritsu Seiyaku Corporation, Tokyo, Japan), and sustained by inhalation anesthesia of isoflurane (Isoflurane, Mairan Pharma, Osaka, Japan). The dorsal hair was shaved to fully expose the skin, which was then rinsed with 70% ethanol. Six full-thickness wounds extending to the panniculus carnosus

were created on each mouse using a 3-mm diameter biopsy punch (Biopsy Punch, Kai Industries Co., Ltd., Gifu, Japan) under sterile conditions. The wounds were covered with a polyurethane film (Tegaderm Transparent Dressing, 3M Health Care, St. Paul, MN, USA) and an elastic adhesive bandage (Hilate, Iwatsuki, Tokyo, Japan) as an occlusive dressing. The day on which the wounds were made was day 0. At various time points, mice were sacrificed and wound tissue was collected by excising the tissue using an 8-mm diameter biopsy punch.

Treatment with dZymosan (zymosan depleted) or α-mannan

dZymosan (zymosan depleted), which was prepared from *Saccharomyces cerevisiae* cell walls treated with hot alkali to remove all their TLR-stimulating properties, was purchased from Invivogen (San Diego, CA, USA) and diluted with phosphate buffered saline (PBS) at 0.5 mg/mL. Mannan from *Saccharomyces cerevisiae* (α-mannan) was purchased from Sigma-Aldrich (St. Louis, MO, USA) and diluted with phosphate buffered saline (PBS) at 10 mg/mL. Wounds were created in accordance with the method described above, and immediately after wounding, a 3-μL suspension of dZymosan (2.5 μg), α-mannan (30 μg), or PBS as a vehicle control was applied to the base of the wounds in WT, Dectin-1KO, or Dectin-2KO mice.

Administration of deoxyribonuclease (DNase) I

DNase I, a deoxyribonuclease for single-stranded DNA and double-stranded DNA, was purchased from FUJIFILM Wako Pure Chemical Co. (Osaka, Japan) and dissolved in normal

saline at a concentration of 250 U/mL. To inhibit single- and double-stranded DNA, WT mice and WT mice treated with α-mannan were injected intraperitoneally with a 200 μL suspension of DNase I (50 U) each day from 1 day before wounding to 1 day before tissue collection. As a control group for the relevant experiments, mice were injected with normal saline at the same time points.

Neutrophil depletion with anti-Gr-1 antibody

Anti-Gr-1 monoclonal antibody was purified from hybridoma culture supernatants (clones RB6-8C5) using a protein G column kit (Kirkegaard & Perry Laboratories, Gaithersburg, MD, USA). This monoclonal antibody (Gr-1) completely depletes mouse neutrophils (Miura et al., 2019). To neutralize the biological activity of neutrophils, mice were injected intraperitoneally with 400 μg of mAb at 24 hours after wounding. Rat IgG (ICN Pharmaceuticals, Aurora, OH, USA) was used as a control antibody.

Measurement of wound areas

Wound areas were measured on digital images that were obtained with a digital camera (CX4; Ricoh, Tokyo, Japan). After the wounds were created, photographs were taken of each wound before dressing. At various time points, the polyurethane films were removed from the mice and the wounds were photographed. Each wounded area was quantified by tracing its margin and calculating the pixel area using AxioVision imaging software, release 4.6 (Carl Zeiss Micro Imaging Japan, Tokyo, Japan). The percentage of wound closure was calculated using the following formula: % wound closure = (1 – wound area at the indicated time point /

wound area 1 on day 0) × 100.

Analysis of hydroxyproline content

Wounds were removed using an 8-mm diameter biopsy punch after mice were sacrificed, and total wound hydroxyproline content was assayed. Briefly, all wound tissue was homogenized and then hydrolyzed in 6N HCl for 21 hours at 120°C. The hydrolysate was neutralized with NaOH. In the next step, 2-mL aliquots were analyzed calorimetrically for hydroxyproline content adding 1 mL of 0.05 mol/L chloramine T (Nacalai Tesque, Kyoto, Japan), 1 mL of 3.15 mol/L perchloric acid (Nacalai Tesque), and 1 mL of 20% dimethylaminobenzaldehyde (Nacalai Tesque). The optical densities of the samples were determined using a spectrophotometer at 557 nm.

Histology and immunohistochemistry

The removed wound tissues were fixed with 4% paraformaldehyde-phosphate buffer solution and embedded in paraffin. Sections were taken from the central portion of the wound and stained with hematoxylin-eosin (HE) in accordance with the standard method. The extent of re-epithelialization in each wound was measured in these HE-stained sections by measuring the distance from the normal wound margin to the edge of the epithelium. The re-epithelialization index was determined based on the percentage of new epithelium that was present in the total wound.

For immunohistochemistry, after blocking with endogenous peroxidase using methanol/ hydrogen peroxide, the sections were incubated with 10% normal rabbit serum for 20 min to

block non-specific binding and then stained with anti-Dectin-1 Ab (dilution 1:25; BioLegend, San Diego, CA, USA), anti-Dectin-2 Ab (dilution 1:100; Bio-Rad Laboratories, Hercules, CA, USA), anti-Vimentin Ab (dilution 1:100; Abcam plc, Cambridge, UK), anti-β-glucuronidase (dilution 1:100; Proteintech, Rosemont, IL, USA), anti-proliferating cell nuclear antigen (PCNA) Ab (dilution 1:100; Agilent Technologies, Santa Clara, CA, USA), anti-α-smooth muscle actin (α-SMA) Ab (dilution 1:300; Vector Laboratories, Inc., Burlingame, CA, USA), and anti-CD31 (PECAM-1) Ab (0.25 μg/mL; Santa Cruz Biotechnology, Santa Cruz, CA, USA). The sections were incubated with peroxidase-conjugated secondary Ab (4 μg/mL; Histofine Simple Stain MAX-PO, Nichirei Bioscience, Tokyo, Japan).

Epithelial cell differentiation, vascular density in the granulation tissue, and myofibroblast differentiation were determined by counting the number of PCNA-positive epithelial cells, the number of CD31-positive vessels, and the number of α-SMA-positive cells, respectively. All analyses were performed under blinded conditions.

For fluorescent immunostaining, the tissues were embedded in OCT compound (Sakura Finetechnical Co., Tokyo, Japan) and quickly frozen. The sections were taken from the central portion of the wound, blocked with 10% normal goat serum (Nichirei Bioscience, Tokyo, Japan), and incubated with a primary Ab against citrullinated histone H3 (Cit H3) (rabbit) (0.04 μg/mL; Abcam) and anti-Ly6G (rat) (clone 1A8, 5 μg/mL; BioLegend) at 4°C overnight, and then with Alexa 488-conjugated secondary Ab (anti-rabbit) (0.02 μg/mL; Life Technologies, Tokyo, Japan) and Alexa 555-conjugated secondary Ab (anti-rat) (0.02 μg/mL; Life Technologies) for 30 min at room temperature (RT). After the sections were covered

with mountant (VECTASHIELD® Hard Set Mounting Medium; Vector Laboratories, Inc.), images were acquired by fluorescence microscopy (FSX100; Olympus, Tokyo, Japan).

Preparation of leukocytes in the wound tissue

Mice were sacrificed at 6, 12, or 24 hours or on days 3, 5, or 7 after wound creation. The wound tissues were excised using a biopsy punch (8 mm in diameter) and teased apart using stainless-steel mesh in RPMI 1640 medium (Nipro, Osaka, Japan) supplemented with 10 mM HEPES, 10% fetal calf serum (FCS) (BioWest, Nuaillé, France), 1 mg/mL collagenase, and 1 mg/mL hyaluronidase (Sigma-Aldrich). They were incubated for 2 hours at 37°C with vigorous shaking. After incubation, the tissue fragments and most dead cells were removed by passing the cells through a 70-μm cell strainer (BD Falcon, Bedford, MA, USA). They were then washed three times with 1% FCS RPMI 1640 medium and used as skin leukocytes for flow cytometric analysis.

Analysis of Dectin-1, 2-positive cells using flow cytometry

The cells obtained from the wound tissues were stained with Pacific blue-anti-CD45 monoclonal antibody (mAb) (clone 30-F11, BioLegend), allophycocyanin cyanin 7 (APC/Cy7)-anti-Ly6G mAb (clone 1A8, BioLegend), phycoerythrin (PE)-anti-F4/80 mAb (clone BM8, BioLegend), allophycocyanin (APC)-anti-CD140a mAb (clone APA5, BioLegend), APC-anti-Dectin-1 mAb (clone RH1, BioLegend), and fluorescein isothiocyanate (FITC)-anti-Dectin-2 mAb (clone KVa7-6E7, Miltenyi Biotec, Bergisch Gladbach, Germany). Isotype-matched irrelevant IgG was used as the control staining.

Macrophages and neutrophils were identified as CD45+F4/80+ cells and CD45+Ly6G+ cells, respectively. Fibroblasts were identified as CD45+CD140a+ cells. The stained cells were analyzed using a BD FACS Canto II flow cytometer (BD Bioscience, San Jose, CA, USA).

Analysis of leukocyte fraction using flow cytometry

The cells obtained from wounded tissues were stained with Pacific blue-anti-CD45 mAb (clone 30-F11, BioLegend), APC-anti-CD11b mAb (clone M1/70, BioLegend), APC/Cy7-anti-Ly6G mAb (clone 1A8, BioLegend), and Alexa Fluor®488-anti-F4/80 mAb (clone BM8, BioLegend). Isotype-matched irrelevant IgG was used for control staining. Macrophages and neutrophils were identified as CD45+CD11b+F4/80+ cells and CD45+CD11b+Ly6G+ cells, respectively. The stained cells were analyzed using a BD FACS Canto II flow cytometer (BD Bioscience). The numbers of neutrophils and macrophages were estimated by multiplying the total leukocyte number by the proportion of each fraction.

RNA extraction and quantitative real-time RT-PCR

Total RNA was extracted from wound tissues using ISOGEN (Nippon Gene Co. Ltd., Tokyo, Japan), and first-strand cDNA was synthesized using a PrimeScript first-strand cDNA synthesis kit (TaKaRa Bio Inc., Otsu, Japan), in accordance with the manufacturer's instructions. Quantitative real-time polymerase chain reaction (PCR) was performed in a volume of 20 μL using gene-specific primers and FastStart essential DNA green master mix (Roche Applied Science, Branford, CT, USA) in a Step One™ (Thermo Fisher, Waltham, MA, USA). Primers were as follows: 5′-CCTTGGAGGCCCATTGC-3′ (Forward) and 5′-

GCAACCACTACTACCACAAAGCA-3′ (Reverse) for Dectin-1; 5′-CTG GAG CAC CAG TGA GCA GAA C-3′ (Forward), and 5′-CCA TTT GCC ATT ACC TTG TGG A-3′ (Reverse) for Dectin-2; 5′-AAG ACA AGG CAG CGG TGG AA-3′ (Forward) and 5′- GCA GGG GAC AGG AAA TAG TT-3′ (Reverse) for COL1A1; 5′-GGA CCA GGC AAT GAT GGA AAA CC-3′ (Forward) and 5′-ACC AGG GAA ACC CAT GAC ACC-3′ (Reverse) for COL3A1; 5′-TAC GCC TGA GTG GCT GTC TTT T-3′ (Forward) and 5′-CGT GGA GTT TGT TAT CTT TGC TGT-3′ (Reverse) for TGF-β; 5′-CCC CTG ATG TCC AGC AAG TAG A-3′ (Forward) and 5′-AGT CTG CGA TGA GCT TAG GGA AA-3′ (Reverse) for MMP-2; 5′-GAT TCA GAA ACG TGG ACT CAA-3′ (Forward) and 5′-CAT CAA GGC ACC AGG ATC AGT-3′ (Reverse) for MMP-8; and 5′-GCT TCC TCA GAC CGC TT-3′ (Forward) and 5′-TCG CTA ATC ACG CTG GG-3′ (Reverse) for β-actin (ACTB). The reaction efficiency with each primer set was determined using standard amplifications. Target gene expression levels and that of ACTB as a reference gene were calculated for each sample using the reaction efficiency. The results were analyzed using a relative quantification procedure and are presented as expression levels relative to ACTB expression.

Measurement of cytokine concentrations

The wound tissues were homogenated with saline solution, and the concentrations of cytokine and chemokine in the supernatants were measured using appropriate enzyme-linked immunosorbent assay (ELISA) kits (BioLegend for TNF-α and IL-17A; R&D Systems for CXCL1, CXCL2, and CCL2). The results were expressed as the values per wound.

Western blot analysis

Frozen skin wound tissues were weighed and homogenized in RIPA buffer (Wako Pure Chemical Industries, Osaka, Japan) supplemented with Protease Inhibitor Cocktail (Sigma-Aldrich) on ice. After centrifugation at 20,000 ×*g* for 20 min at 4°C, the protein concentration was determined using the bicinchoninic acid method (Pierce Biotechnology, Rockford, IL, USA). An equal amount of protein per sample was separated by SDS-PAGE using gradient gels (4–20% Tris-Glycine gels, Bio-Rad Laboratories) and transferred to polyvinylidene difluoride membranes (ATTO Corporation, Tokyo, Japan) using a semidry transblot system (ATTO Corporation). Non-specific binding on the blots was blocked with 0.5% (w/v) skim milk and 0.1% (v/v) Tween 20 in TBS for 2 hours at RT, followed by incubation for 1 hour at RT with primary antibodies (rabbit polyclonal anti-Cit H3, 1:1000, Abcam; rabbit polyclonal anti-H3, 1:2000, cell signaling; mouse anti-GAPDH, 1:2000, MBL, Nagoya, Japan) overnight at 4°C. Blots were incubated with appropriate HRP-conjugated secondary antibodies (goat anti-rabbit IgG, 1:5000, cell signaling; goat anti-mouse IgG, 1:5000, cell signaling) for 1 hour at RT. The blots were developed with enhanced chemiluminescence substrate (Nacalai Tesque, cat. no. 11644). Chemiluminescent signals were detected using ImageQuant LAS 4000 analyzer (FujiFilm, Tokyo, Japan). Blots were quantified using ImageJ software.

Measurement of neutrophil elastase activity

The wound tissue was homogenized with PBS, and the concentration of elastase activity was measured using the EnzChek Elastase Assay Kit (Thermo Fisher), in accordance with the manufacturer's instructions. The results were expressed as the values per wound. The

detection limit was 0.004 U/mL.

Preparation of skin supernatant using wounded tissues and Dectin-1- and Dectin-2-NFAT–GFP reporter assay

Mice were sacrificed at 24 hours after wound creation. The wounded tissues were excised using a biopsy punch (8 mm in diameter) and the tissue from six wounds was homogenized in 2 mL of RPMI 1640 medium using stainless-steel mesh. After homogenization, most dead cells were removed by passing the cells through an 8-μm cell strainer (BD Falcon).

T cell hybridoma 2B4 cells were transfected with the NFAT-GFP construct prepared by fusing three tandem NFAT-binding sites with enhanced GFP cDNA (Ohtsuka et al., 2004). This cell line was transfected with Dectin-1 or Dectin-2 and FcRγ genes, and the same cell line lacking Dectin-1 or Dectin-2 was used as a control. These cells were stimulated with the above-mentioned skin supernatant or 60 μg/mL dZymosan for Dectin-1 reporter cells, or 3 mg/mL α-mannan for Dectin-2 reporter cells as a positive control, for 20 hours. Additionally, 10% FCS RPMI 1640 medium was used as a control medium. After the stimulation, these cells were stained with allophycocyanin (APC)-anti-CD3 mAb. GFP expression was analyzed in the CD3+ cells but not in the dead 7-aminoactinomycin D (7-AAD)-stained cells by flow cytometry.

Statistics

Data are expressed as the mean ± standard deviation (SD). Data analysis was performed using Welch's *t*-test to compare two experimental groups, and a one-way ANOVA with post-hoc

Dunnett's or Turkey–Kramer's honestly significant difference (HSD) test was used for more than three experimental groups. A p value less than 0.05 was considered to indicate significance.

Study approval

All experimental protocols described in the present study were approved by the Ethics Review Committee for Animal Experimentation of Tohoku University and performed in accordance with institutional ethical guidelines.

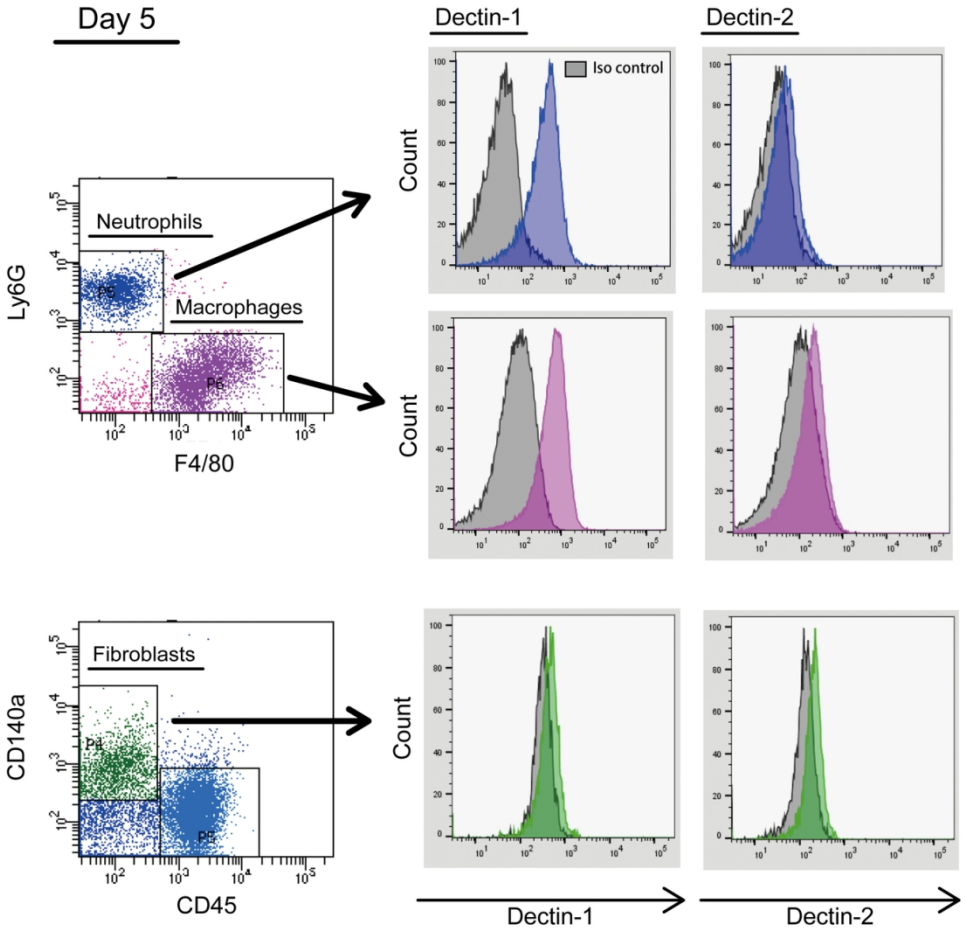

119x117mm (300 x 300 DPI)

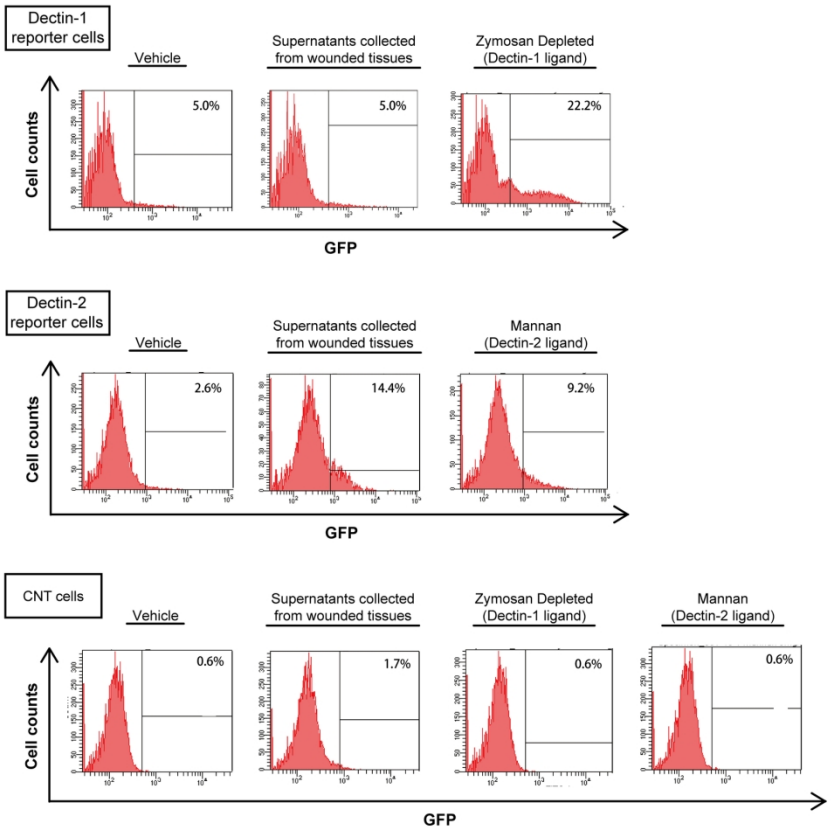

175x160mm (300 x 300 DPI)

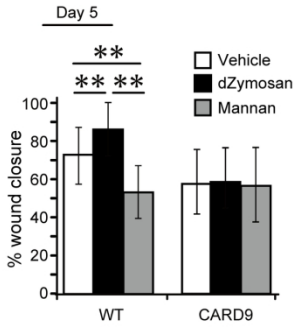

174x99mm (300 x 300 DPI)

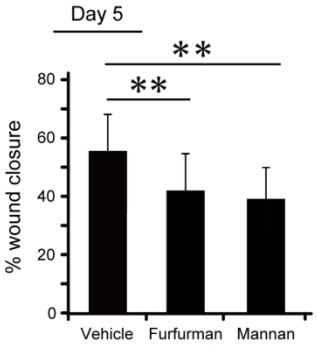

174x93mm (300 x 300 DPI)

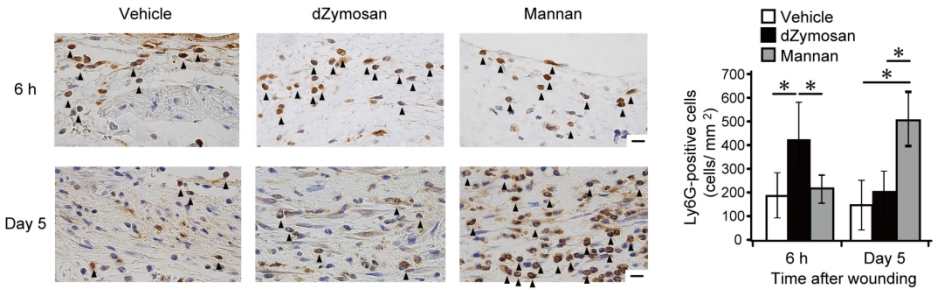

175x75mm (300 x 300 DPI)

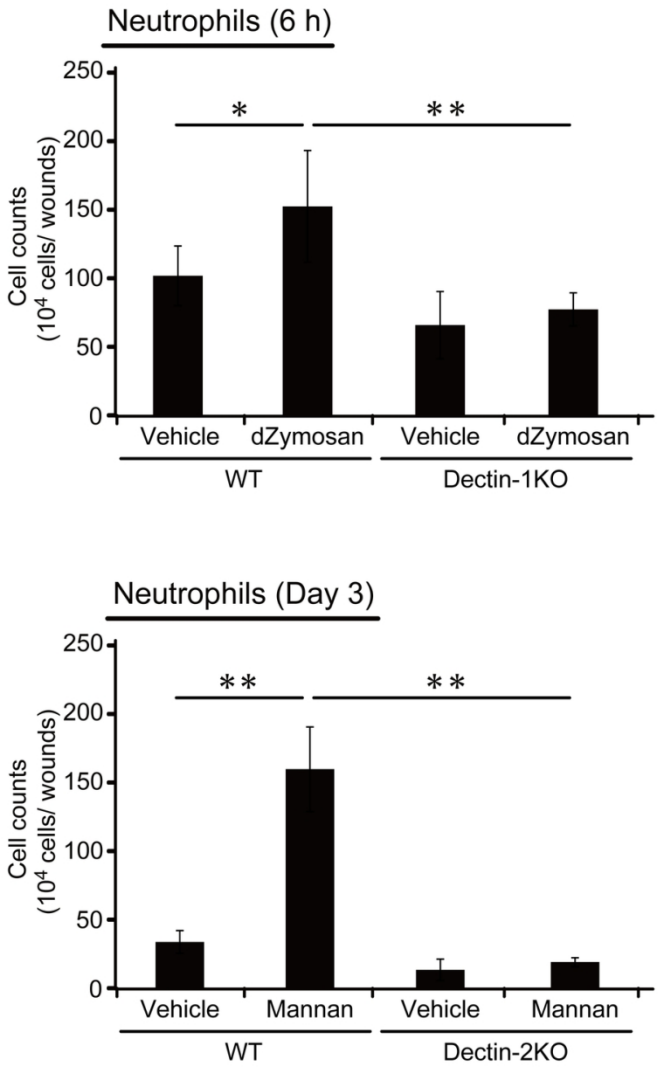

90x139mm (300 x 300 DPI)

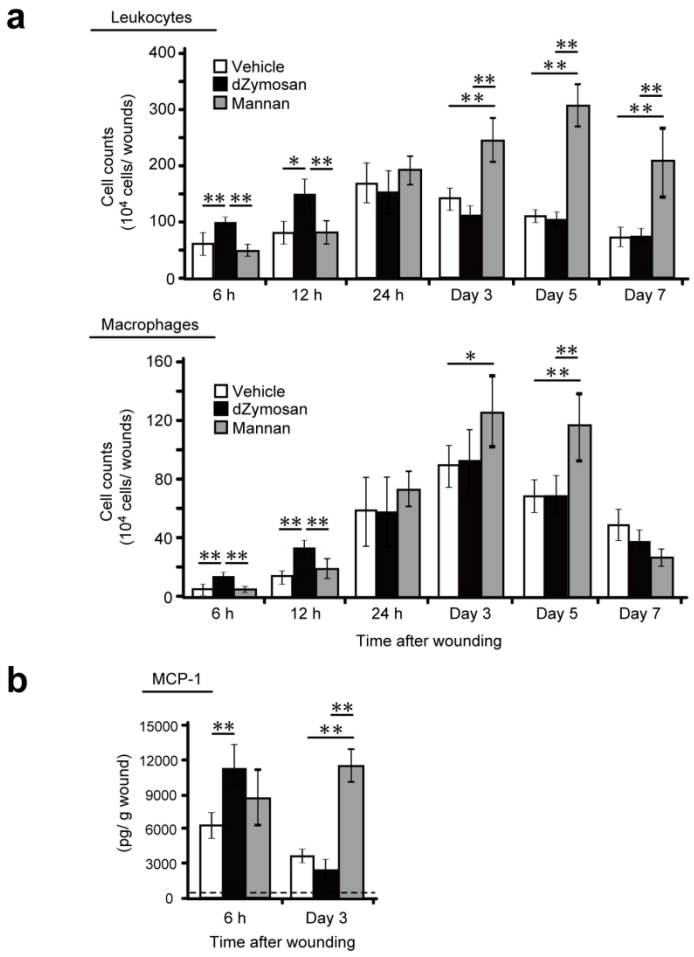

175x179mm (300 x 300 DPI)

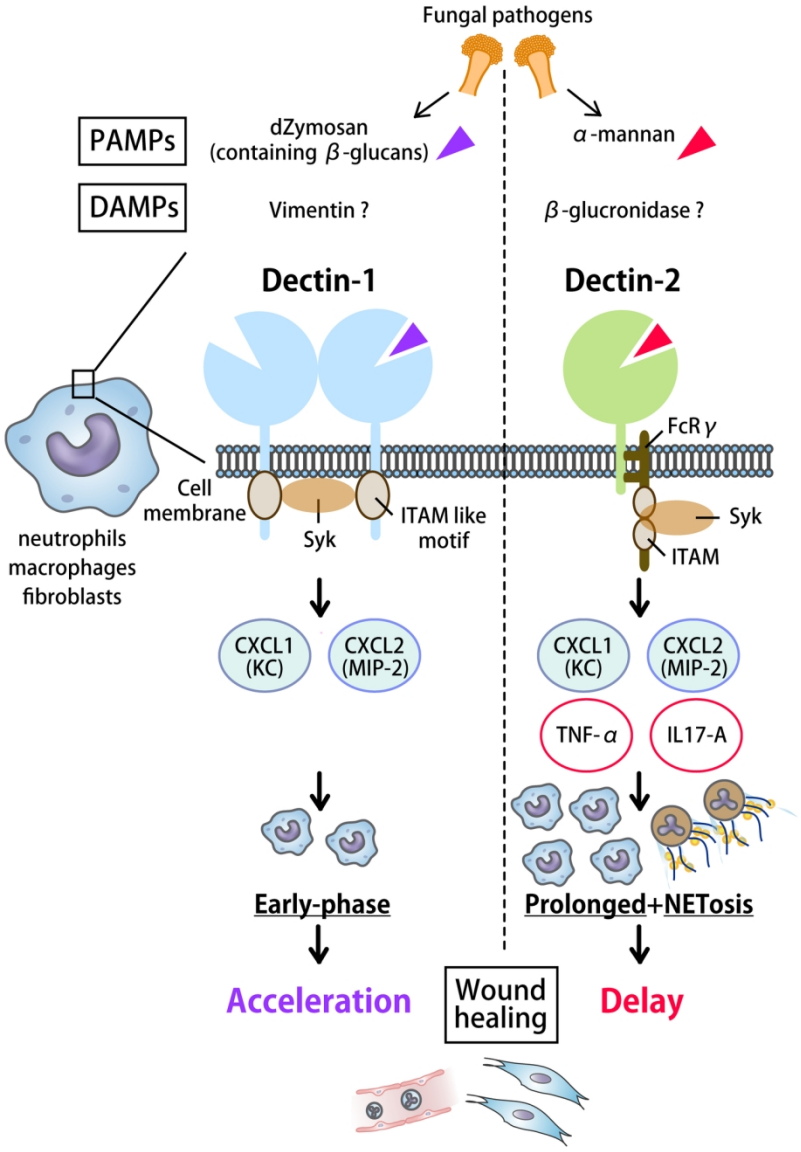

142x183mm (300 x 300 DPI)